Effective magnetic properties of arrays of interacting ferromagnetic wires exhibiting gyromagnetic anisotropy and retardation effects

Vincent Boucher* and David Ménard†

Département de Génie Physique, Regroupement Québécois sur les Matériaux de Pointe (RQMP), École Polytechnique de Montréal, CP 6079, Succ. Centre-ville, Montréal, Québec, Canada H3C 3A7

(Received 9 February 2010; published 6 May 2010)

We present a model for the effective magnetic properties of metamaterials composed of gyromagnetic inclusions in which electromagnetic retardation is accounted for. The formalism is used to derive the effective permeability tensor of axially magnetized ferromagnetic-metallic wires. The complex size-dependent gyromagnetic response of a single wire subjected to an external dynamic magnetic field is first obtained and expressed compactly in terms of renormalized permeability components. We then incorporate this response into an extended Maxwell-Garnett homogenization procedure to yield the effective permeability tensor of the array. An effective external susceptibility tensor, which includes dipolar interactions explicitly, is further introduced to describe the ferromagnetic resonance response of finite-size arrays placed in microwave resonant cavities. We examine the impact of electromagnetic retardation on the resonance, antiresonance, and linewidth and compare the magnetic response expected for conducting and insulating magnetic wires. The conditions under which arrays of ferromagnetic wires may exhibit a region of negative effective permeability are established and are found to be dependent on both the intrinsic magnetic and size-dependent eddy-current losses, thus providing useful guidelines for the design of magnetic metamaterials. The proposed formalism is sufficiently general to be applied or extended to various systems of interest.

DOI: 10.1103/PhysRevB.81.174404 PACS number(s): 75.75.Jn, 76.50.+g, 41.20.Jb

I. INTRODUCTION

Electromagnetic metamaterials consist of effectively homogeneous artificial composite materials exhibiting response functions and dispersion relations not readily accessible to conventional materials. They are typically synthesized by embedding conducting or high-permittivity subwavelength inclusions of specific composition and geometry (e.g., size, shape, spacing, and arrangement) into a host matrix. Their development has sparked considerable interest in the last decade, owing to the exciting possibilities they bring to microwave and optical technologies.[1–4] Recent proposals for the use of ferromagnetic inclusions exhibiting simultaneous gyromagnetic and dispersive intrinsic magnetic responses at microwave frequencies have opened the way to a new class of metamaterials with magnetic-field-tunable effective constitutive parameters.[5–10] These *magnetic* metamaterials may provide significant advantages over first-generation metamaterials consisting of combined arrays of wires[11,12] and split-ring resonators,[13,14] that is, nonmagnetic resonant metallic inclusions with geometry-dependent parameters and limited external tunability. In particular, composites based on ferromagnetic-metallic wires have been the focus of several studies due to their potential in microwave devices,[15–20] electromagnetic wave absorbers,[21,22] magneto-optical applications,[23,24] and as candidates for left-handed materials with both negative effective permittivity and permeability.[25–30] Likewise, the microwave response of arrays of interacting ferromagnetic nanowires has been studied extensively and has been shown to support both a uniform mode of precession[31–35] and dipole-exchange spin-wave excitations.[36–39]

Exploiting the full technological potential of these effective magnetic media requires theoretical models able to predict their macroscopic electromagnetic response. The main challenge in developing such models consists in properly incorporating the rich microwave dispersion relation exhibited by ferromagnetic-metallic inclusions, which is governed primarily by two distinct mechanisms: the gyromagnetic resonant precession of the magnetization and the skin effect (SE). On the one hand, the intrinsic permeability is a gyrotropic tensor property with complex diagonal and off-diagonal components exhibiting a resonant behavior with frequency and static magnetic field. It is characterized by the ferromagnetic resonance (FMR), ferromagnetic antiresonance (FMAR), and by a linewidth due to intrinsic magnetic losses.[40] On the other hand, irrespective of its intrinsic magnetic properties, a metallic body subjected to a high-frequency magnetic field acquires a magnetization, owing to the generation of eddy currents within the skin depth.[41] This leads to a $k_i a$-dependent diamagnetic response accompanied by resistive losses, where k_i is the wave vector inside the individual inclusions of characteristic size a. In ferromagnetic metals at microwave frequencies, the gyromagnetic nature of the intrinsic permeability manifests itself in the dispersive behavior of k_i, which in turn modifies the lossy diamagnetic response set up by the eddy currents. Ferromagnetic and metallic dispersions and dissipations (losses) are thus closely linked, the coupling being strongest when the FMR frequency approaches the frequency at which the skin depth is comparable to the size of the inclusions. In this regime, the scattering response of gyromagnetic-metallic inclusions is characterized by size-dependent FMR and FMAR frequencies and by a linewidth determined by the combined effect of magnetic and conduction losses.[42,43]

Several features and complications arising from this dual ferromagnetic-metallic response have not been fully incorporated into existing models for the electromagnetic properties

of magnetic metamaterials. The macroscopic behavior of a composite material is usually related to the scattering response of the individual inclusions by effective constitutive parameters derived from effective-medium theories, most notably the Maxwell-Garnett and the Bruggeman formalisms.[44] In their simplest and usual formulations, these mixing rules are derived within the quasistatic (QS) approximation, which assumes that the time-varying fields inside the inclusions are spatially uniform. In this context, various authors have proposed expressions for the effective permeability tensor $\overleftrightarrow{\mu}_{\text{eff}}$ of composite materials made of gyromagnetic inclusions excited in the uniform precession mode.[8,16,27,45–47] However, the skin depth in metals may fall below 1 μm at microwave frequencies, which leads to propagation and attenuation of the fields throughout the volume of the conductor, thereby invalidating the use of QS theories.

A way to overcome this difficulty was first proposed by Lewin for the case of a cubic lattice of spherical inclusions with complex *scalar* permittivity and permeability.[48] Based on the Mie scattering theory, his work introduces $k_i a$-dependent renormalized expressions for the permittivity and permeability of the individual inclusions, which account for retardation effects and yield compact Maxwell-Garnett-type formulas for the effective electromagnetic properties of the medium. This approach was subsequently extended by Khizhnyak to scatterers of arbitrary shape[49] and to two-dimensional arrays of infinite rods[50] but has not been generalized to the case of inclusions with anisotropic (e.g., gyrotropic) properties. Nevertheless, Lewin's theory has been used over the last two decades to yield the effective permeability of various systems formed of magnetic particles,[51–60] thus incorporating electromagnetic retardation but neglecting the gyromagnetic response of the individual inclusions. This issue has been considered in a recent study of the effective constitutive parameters of a magnetic metamaterial consisting of insulating ferrimagnetic rods.[10] However, although the authors of Ref. 10 incorporate both the gyromagnetic and $k_i a$-dependent responses of the individual rods, their model results in an effective *scalar* permeability, which is restricted to one specific mode of wave propagation within arrays of infinite lateral extent. In particular, their implicit assumption of unbounded samples, which is made in most existing theories for the electromagnetic response of magnetic composite materials, prevents a proper account of dipolar interactions created by surface poles in finite-size samples.

In this work, we propose a multiscale effective-medium theory that addresses most of the difficulties mentioned above, arising from the presence of interacting ferromagnetic inclusions in a composite of finite extent. The formalism is used to derive the effective permeability tensor $\overleftrightarrow{\mu}_{\text{eff}}$ of arrays of axially magnetized ferromagnetic-metallic wires, each characterized by a *gyromagnetic* permeability tensor, under circumstances where the skin effect in the individual wires cannot be neglected. The emphasis is put on the influence of electromagnetic retardation and of the geometrical parameters of the array on the FMR, FMAR, and linewidth of the effective permeability spectrum. This allows us to study the conditions leading to a region of negative effective permeability in the interval between the FMR and FMAR, which is required for left-handed materials. We also examine the trade-off between the design flexibility permitted by ferromagnetic-metallic inclusions and the limitations imposed by their intrinsic losses.

The paper is structured as follows. Section II establishes the electromagnetic response of a single ferromagnetic-metallic wire described by the gyromagnetic permeability tensor $\overleftrightarrow{\mu}_w$ with diagonal and off-diagonal components μ and μ_t and intrinsic magnetic losses accounted for by a phenomenological Gilbert damping term. We consider the scattering by an axially magnetized wire of radius a excited by a plane wave with both its wave vector and magnetic-field component oriented transverse to the wire axis. Introducing the size-dependent external susceptibility tensor $\overleftrightarrow{\eta}_w$ allows us to express the field scattered by the wire as a two-dimensional dipolar field. A key result of the paper is Eq. (26) for the diagonal and off-diagonal components $\tilde{\eta}$ and $\tilde{\eta}_t$ of $\overleftrightarrow{\eta}_w$, which have a compact form in terms of $k_w a$-dependent renormalized permeability components $\tilde{\mu}$ and $\tilde{\mu}_t$, where k_w is the wave vector inside the wire. Our approach thus extends Lewin's theory to cylindrical inclusions with a gyromagnetic permeability tensor and recovers several known results in the limits of weak and strong skin effect.

In Sec. III, we incorporate our expression for $\overleftrightarrow{\eta}_w$ into the Maxwell-Garnett homogenization procedure, in order to derive the effective permeability tensor $\overleftrightarrow{\mu}_{\text{eff}}$ of the wire array [Eq. (50)]. Our expression for $\overleftrightarrow{\mu}_{\text{eff}}$ describes the effective magnetic properties of the array and accounts for the gyrotropic and lossy response of the wires, including skin effect, as well as for the influence of the geometrical parameters on the intrawire shape demagnetizing and static interwire dipolar interactions. The FMR response of a finite-size array is obtained next in Sec. IV. There, we introduce the effective external susceptibility tensor $\overleftrightarrow{\eta}_{\text{eff}}$, to be distinguished from the effective permeability $\overleftrightarrow{\mu}_{\text{eff}}$, along with an effective demagnetizing tensor $\overleftrightarrow{N}_{\text{eff}}$ related to the formalism used in Ref. 35 and based on an explicit account of dipolar interactions.

Section V presents theoretical results of our model and a discussion of the dependence of the magnetic response of the wire on $k_w a$, as well as on the dielectric nature of the wire (conducting or insulating). The effective permeability of an array of ferromagnetic wires is also studied, with particular emphasis on the possibility of obtaining a negative response. Finally, Sec. VI outlines the significance and limitations of the present work, suggests some possible extensions of the theory and summarizes our main results.

II. DYNAMIC RESPONSE OF A SINGLE FERROMAGNETIC WIRE

The effective magnetic properties of an ensemble of inclusions, as derived from the homogenization procedure presented in Sec. III, is built upon the response of a single inclusion, which is established in this section. Therefore, we first consider a single ferromagnetic-metallic wire embedded in a nonmagnetic dielectric matrix and subjected to a harmonic electromagnetic plane wave of angular frequency ω in the microwave frequency range. The dynamic magnetization response of the wire is investigated as a function of the incident microwave magnetic field, under circumstances where

electromagnetic retardation inside the wire plays a significant role, so that the magnetic response exhibits nontrivial size dependence.

A. Intrinsic electromagnetic response of a single ferromagnetic wire

The isotropic local permittivity of the wire is given by $\epsilon_w = i\sigma_w/\omega$, where σ_w is the static Drude conductivity. This expression thus ignores galvanomagnetic responses, such as Hall effect and magnetoresistance, neglects displacement currents compared to conduction currents, and assumes that the Drude relaxation time $\tau \ll 1/\omega$. The large and imaginary dielectric response leads to a finite penetration of the electromagnetic fields within the wire, which is characterized by the nonmagnetic skin depth,

$$\delta_{w0} = \sqrt{\frac{2}{\omega\sigma_w\mu_0}}, \tag{1}$$

where μ_0 is the permeability of free space.

Neglecting the exchange interaction and magnetocrystalline anisotropy, the intrinsic permeability tensor $\vec{\vec{\mu}}_w$ of the wire establishes a local relation between the dynamic magnetic field and induction within the wire,

$$\mathbf{b}_w = \vec{\vec{\mu}}_w \mathbf{h}_w. \tag{2}$$

To obtain $\vec{\vec{\mu}}_w$, we must solve the linearized Landau-Lifshitz-Gilbert equation of motion for the magnetization $\mathbf{M}_w = \mathbf{M}_{w0} + \mathbf{m}_w$ of the wire, subject to the internal field $\mathbf{H}_w = \mathbf{H}_{w0} + \mathbf{h}_w$. We assume that the dynamic components $\mathbf{m}_w$ and $\mathbf{h}_w$ have a harmonic time dependence of the form $e^{-i\omega t}$ and are oriented perpendicular to the static components $\mathbf{M}_{w0} = M_s\hat{\mathbf{z}}$ and $\mathbf{H}_{w0} = H_{w0}\hat{\mathbf{z}}$, where M_s is the saturation magnetization. This yields the gyromagnetic permeability tensor[40]

$$\vec{\vec{\mu}}_w = \mu_0(\vec{\vec{I}} + \vec{\vec{\chi}}_w) = \begin{pmatrix} \mu & -i\mu_t & 0 \\ i\mu_t & \mu & 0 \\ 0 & 0 & \mu_0 \end{pmatrix}, \tag{3}$$

where $\vec{\vec{I}}$ is the identity matrix, $\vec{\vec{\chi}}_w$ is the intrinsic susceptibility tensor of the wire satisfying

$$\mathbf{m}_w = \vec{\vec{\chi}}_w \mathbf{h}_w \tag{4}$$

and

$$\mu = \mu_0 \frac{\omega_H^*(\omega_H^* + \omega_M) - \omega^2}{(\omega_H^*)^2 - \omega^2}, \quad \mu_t = \mu_0 \frac{\omega_M \omega}{(\omega_H^*)^2 - \omega^2} \tag{5}$$

are the diagonal and off-diagonal components of $\vec{\vec{\mu}}_w$, with

$$\omega_H^* = \omega_H - i\alpha\omega = \mu_0|\gamma|H_{w0} - i\alpha\omega, \tag{6}$$

$$\omega_M = \mu_0|\gamma|M_s. \tag{7}$$

Here, α is the Gilbert damping constant and $-|\gamma| = -g\mu_B/\hbar$ is the gyromagnetic ratio, where g is the spectroscopic splitting factor, μ_B is the Bohr magneton, and $\hbar$ is the Planck constant divided by 2π. The effect of neglecting the exchange interaction and magnetocrystalline anisotropy will be discussed and justified in Sec. VI.

The intrinsic tensor $\vec{\vec{\mu}}_w$ in Eq. (3) yields the magnetic response of the material to the internal field, regardless of the shape and size of the sample. The complex components μ and μ_t depend on the value of the saturation magnetization M_s and account for magnetic losses via the phenomenological Gilbert damping constant α. They exhibit a resonant dependence on frequency and static magnetic field, with a pole and a zero corresponding to the FMR and FMAR frequencies, respectively. The magnetic response for some particular experimental configuration is generally obtained by using $\vec{\vec{\mu}}_w$ in Maxwell's equations and by solving the appropriate boundary-value problem.

B. External magnetic response of a single ferromagnetic wire

Consider now that the ferromagnetic wire is subjected to a uniform local dynamic magnetic field $\mathbf{h}_{\text{loc}}$, such as that produced in a microwave resonant cavity. In FMR experiments involving a sufficiently small wire, perturbation theory is assumed to hold.[40] In such a case, the quantity proportional to the measured shifts in resonance frequency and quality factor due to the response of the sample is the external susceptibility tensor $\vec{\vec{\eta}}_w$,[40,61] defined here as

$$\langle \mathbf{m}_w \rangle = \vec{\vec{\eta}}_w \mathbf{h}_{\text{loc}}, \tag{8}$$

where $\langle \mathbf{m}_w \rangle$ is the volume average of the nonuniform magnetization of the wire and $\mathbf{h}_{\text{loc}}$ is the uniform local field imposed on the wire (e.g., the field of an unperturbed cavity mode). Note that the external susceptibility tensor is directly related to the polarizability tensor $\vec{\vec{\alpha}}_w$ of the wire of volume V_w and magnetic dipolar moment $V_w\langle \mathbf{m}_w \rangle = \vec{\vec{\alpha}}_w \mathbf{h}_{\text{loc}}$ and thus corresponds to the magnetic polarizability per unit volume of the wire.

The external susceptibility tensor depends on the intrinsic permeability tensor $\vec{\vec{\mu}}_w$ as well as the shape, size, and orientation of the sample with respect to the exciting field $\mathbf{h}_{\text{loc}}$. In the most general case, a closed-form analytical solution for $\vec{\vec{\eta}}_w$ is not possible. However, depending on the importance of electromagnetic propagation effects inside and outside the wire, we may obtain approximate solutions, corresponding to the three regimes of operation illustrated in Fig. 1(a): QS, extended quasistatic (EQS), and SE.

The QS approximation assumes that both the dynamic fields inside and outside the wire remain uniform over the scale of its radius,[62,63] corresponding to the conditions

$$|k_m|a \ll 1, \tag{9}$$

$$|k_w|a \ll 1, \tag{10}$$

where k_m and k_w are the wave vectors in the matrix and in the wire of radius a, respectively. The external susceptibility tensor then satisfies Eq. (8) in the limit $\langle \mathbf{m}_w \rangle = \mathbf{m}_w$, which corresponds to uniform-mode oscillations in small ellipsoidal samples.[40] In this limit, also referred to as the Rayleigh limit,[44] the size-independent dynamic magnetic response is determined solely by the intrinsic permeability $\vec{\vec{\mu}}_w$ and by the shape of the wire,[64] the latter being accounted for by the demagnetizing tensor $\vec{\vec{N}}_w$, defined below in Eq. (31).

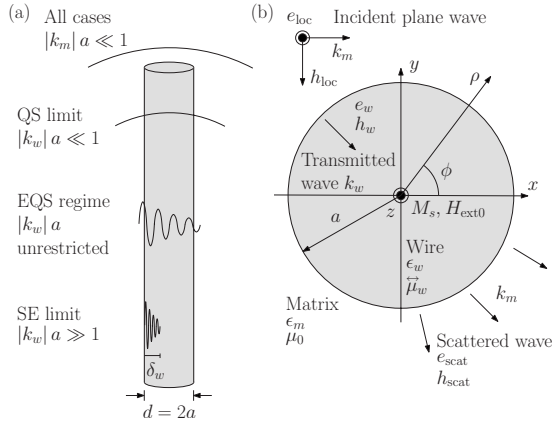

FIG. 1. (a) Schematic representation of the different levels of approximation describing the response of a ferromagnetic wire subjected to a uniform ($|k_m|a \ll 1$) time-varying magnetic field: QS limit with $|k_w|a \ll 1$, EQS regime with $|k_w|a$ unrestricted, and SE limit with $|k_w|a \gg 1$. (b) Definition of the coordinate systems and field parameters related to the problem of the scattering of a plane wave by a ferromagnetic-metallic wire.

The condition $|k_m|a \ll 1$ is easily satisfied over the ranges of frequency (1–100 GHz) and wire radius (0.01–100 μm) considered in this work. Henceforth, we will assume that the local field $\mathbf{h}_{\rm loc}$ imposed on the wire is uniform and thus that Eq. (9) is always fulfilled. However, Eq. (10), which implies a uniform field inside the wire, represents a much more stringent requirement for ferromagnetic-metallic wires. Indeed, the large imaginary permittivity and the enhancement of the permeability near the FMR frequency lead to electromagnetic propagation with $|k_w| \gg |k_m|$ and to a finite penetration depth $\delta_w \propto 1/\mathrm{Im}[k_w]$ of the fields. Further, when the skin depth is such that the condition $|k_w|a \gg 1$ also holds, the dynamic fields remain confined at the wire surface and the SE limit is reached, which is characterized, as the QS limit, by size-independent FMR parameters. However, there exists a range for a in which neither $|k_w|a \ll 1$ nor $|k_w|a \gg 1$ are satisfied so that the external magnetic response depends nontrivially on the product $k_w a$ and thus on the size of the wire.[42,43] This unrestricted case will hereafter be designated as the EQS regime.[65]

In this work, the EQS regime represents the most general situation, which encompasses the QS and SE approximations as limiting cases. We also emphasize that the extended quasistatic terminology can be misleading, as no restriction is imposed on the value of $|k_w|a$. It thus constitutes a fully dynamical calculation of the internal fields, which only assumes that the external field $\mathbf{h}_{\rm loc}$ incident on the wire is uniform.

C. Plane-wave scattering response in the extended quasistatic regime

We now treat the scattering of a plane wave by the axially magnetized ferromagnetic wire embedded in an isotropic matrix of permittivity ϵ_m and permeability $\mu_m = \mu_0$. The scattering configuration is shown in Fig. 1(b). The wire of diameter $d = 2a$ and length L (assumed to be infinite in the scattering problem) is centered at the origin of both a rectangular (x,y,z) and a cylindrical (ρ,ϕ,z) coordinate systems, with its axis parallel to the z axis. For a long wire with negligible axial demagnetizing field, the external static field $\mathbf{H}_{\rm ext0} = H_{\rm ext0}\hat{\mathbf{z}}$ is equal to the internal static field $\mathbf{H}_{w0}$.

The incident wave travels in the $+x$ direction with angular frequency ω and field components

$$\mathbf{e}_{\rm loc} = e_{\rm loc0} e^{i(k_m x - \omega t)} \hat{\mathbf{z}}, \tag{11}$$

$$\mathbf{h}_{\rm loc} = -\frac{e_{\rm loc0}}{\zeta_m} e^{i(k_m x - \omega t)} \hat{\mathbf{y}} = -h_{\rm loc0} e^{i(k_m x - \omega t)} \hat{\mathbf{y}}, \tag{12}$$

where $k_m = \omega\sqrt{\epsilon_m \mu_0}$ and $\zeta_m = \sqrt{\mu_0/\epsilon_m}$ are the wave vector and wave impedance in the matrix. Upon reaching the wire, the incident wave is partly reflected and partly transmitted according to the boundary conditions imposed by Maxwell's equations at the wire surface $\rho = a$. The scattered wave has wave vector k_m while the transmitted wave propagates radially inside the wire, perpendicular to the direction of static magnetization, with wave vector k_w and wave impedance ζ_w given by

$$k_w = \omega\sqrt{\epsilon_w \mu_\perp} = \left(\frac{1+i}{\delta_{w0}}\right)\sqrt{\frac{\mu_\perp}{\mu_0}}, \tag{13}$$

$$\zeta_w = \sqrt{\frac{\mu_\perp}{\epsilon_w}} = \left(\frac{1-i}{\sigma_w \delta_{w0}}\right)\sqrt{\frac{\mu_\perp}{\mu_0}}, \tag{14}$$

where

$$\mu_\perp = \frac{\mu^2 - \mu_t^2}{\mu} = \mu_0 \frac{(\omega_H^* + \omega_M)^2 - \omega^2}{\omega_H^*(\omega_H^* + \omega_M) - \omega^2} \tag{15}$$

is the effective scalar permeability corresponding to this magnetic mode. The scattered and transmitted magnetic fields are both polarized transverse to the wire axis and can be written as infinite sums of orthogonal cylindrical modes with amplitude coefficients a_n and b_n, respectively. The treatment which yields a_n and b_n is straightforward and is presented in Appendix A. Our analysis of the scattering problem draws from earlier studies of FMR in wires under conditions of arbitrary skin effect,[42,43] which we expand by deriving compact and explicit expressions for the diagonal and off-diagonal components of the external susceptibility tensor $\vec{\vec{\eta}}_w$ of the wire.

Under our assumption that $|k_m|a \ll 1$ holds the coefficients of orders $n = 0$ and ± 1 dominate the scattering response[42] so that the main contribution to the scattered wave is the induced dipolar response of the wire. The relative importance of the corresponding modes $n = 0$ and $n = \pm 1$ is governed by the experimental configuration of the exciting field $\mathbf{h}_{\rm loc}$.[43]

In the context of FMR cavity measurements with the wire located at a point of zero electric field and at a maximum of the microwave magnetic field, which is linearly polarized transverse to the wire axis, the mode $n = \pm 1$ is excited predominantly so that only the coefficients $a_{\pm 1}$ and $b_{\pm 1}$ need to be retained. In contrast, when the wire axis is parallel to the microwave electric field, in a region of zero magnetic field, the mode $n = 0$ is excited by the circumferential magnetic

field induced by the resulting electric current. This corresponds to the longitudinal magnetoimpedance configuration.[66] Finally, when the magnetic mode propagates in a transmission line configuration in which the electric and magnetic fields imposed on the wire are simultaneously nonzero, then both the $n=0$ and $n=\pm 1$ modes are required in a proper electromagnetic analysis.

D. Dynamic response to a transverse magnetic field: Mode $n=\pm 1$

In this section, we derive the external susceptibility tensor $\vec{\vec{\eta}}_w$ in the mode $n=\pm 1$ of transverse magnetic excitation, which describes the dipolar response of the wire with equivalent magnetic dipole per unit volume $\langle \mathbf{m}_w \rangle$. It also constitutes the relevant mode in the derivation of the effective permeability,[67] as presented in Sec. III for an array of ferromagnetic wires. Our goal is to express the components of $\vec{\vec{\eta}}_w$ compactly in a form identical to that valid in the QS limit.[40,68] The procedure will consist in defining the $k_w a$-dependent renormalized permeability components $\tilde{\mu}$ and $\tilde{\mu}_t$, then substituting them in place of μ and μ_t, wherever these appear in the QS results.

Outside the wire, the field in the matrix has wave vector k_m and is a superposition of the incident and scattered fields

$$\mathbf{h}_m = \mathbf{h}_{\mathrm{loc}} + \mathbf{h}_{\mathrm{scat}}. \tag{16}$$

In the limits $|k_m|\rho \ll 1$ and $|k_m|a \ll 1$, all Bessel and Hankel functions and their derivatives in Eqs. (A3) and (A5) with $n=\pm 1$ and argument $k_m\rho$ or $k_m a$ may be replaced by their series expansions given in Appendix A, leading to approximate expressions for the incident and scattered fields.

First, the incident field acting on the wire reduces to

$$\mathbf{h}_{\mathrm{loc}} = -h_{\mathrm{loc}0}e^{-i\omega t}\hat{\mathbf{y}} = -h_{\mathrm{loc}}\hat{\mathbf{y}}, \tag{17}$$

where the time dependence is now absorbed into $h_{\mathrm{loc}} = h_{\mathrm{loc}0}e^{-i\omega t}$. As expected, this mode corresponds to a uniform local field, linearly polarized transverse to the wire axis, which could have been obtained directly by setting $k_m=0$ in Eq. (12).

Second, the scattered field excited by $\mathbf{h}_{\mathrm{loc}}$ becomes

$$\mathbf{h}_{\mathrm{scat}} = \frac{2}{\pi(k_m\rho)^2}[(a_1 e^{i\phi} - a_{-1}e^{-i\phi})\hat{\boldsymbol{\rho}} - i(a_1 e^{i\phi} + a_{-1}e^{-i\phi})\hat{\boldsymbol{\phi}}]h_{\mathrm{loc}}, \tag{18}$$

where the scattering coefficients

$$a_{\pm 1} = i\pi\left(\frac{k_m a}{2}\right)^2\left[\frac{\tilde{\mu}^2 - (\tilde{\mu}_t \mp \mu_0)^2}{(\tilde{\mu}+\mu_0)^2 - \tilde{\mu}_t^2}\right] \tag{19}$$

are expressed compactly in terms of *renormalized* permeability components, modified from their intrinsic values due to electromagnetic retardation. We define these as

$$\tilde{\mu} = \mu\left[\frac{(1-\beta^2)G(k_w a)}{1-\beta^2 G^2(k_w a)}\right], \tag{20a}$$

$$\tilde{\mu}_t = \mu_t\left[\frac{(1-\beta^2)G^2(k_w a)}{1-\beta^2 G^2(k_w a)}\right] = \tilde{\mu}\beta G(k_w a), \tag{20b}$$

where $\beta=\mu_t/\mu$,

$$G(k_w a) = \frac{F(k_w a)}{1-F(k_w a)}, \tag{21}$$

$$F(k_w a) = \frac{J_1(k_w a)}{k_w a J_0(k_w a)}, \tag{22}$$

and $J_0(k_w a)$ and $J_1(k_w a)$ are Bessel functions of the first kind. The significance of $\tilde{\mu}$ and $\tilde{\mu}_t$ will become apparent below, when we derive our expression for $\vec{\vec{\eta}}_w$. As in Eq. (15), we may define the permeability component

$$\tilde{\mu}_\perp = \frac{\tilde{\mu}^2 - \tilde{\mu}_t^2}{\tilde{\mu}} = \mu_\perp G(k_w a), \tag{23}$$

which has a simpler form than $\tilde{\mu}$ and $\tilde{\mu}_t$ since it is $\mu_\perp$ that enters k_w and ζ_w, and thus that governs wave propagation inside the wire.

Now, based on the fact that the local field excites a dipolar response from the wire,[65,69] the EQS scattered field in Eq. (18) can also be written as the two-dimensional dipolar field generated by a point dipole at the origin, with equivalent magnetic moment per unit volume $\langle \mathbf{m}_w \rangle$. This yields

$$\mathbf{h}_{\mathrm{scat}} = \frac{a^2}{2\rho^2}[2(\langle \mathbf{m}_w \rangle \cdot \hat{\boldsymbol{\rho}})\hat{\boldsymbol{\rho}} - \langle \mathbf{m}_w \rangle]$$

$$= \frac{a^2}{2\rho^2}[2(\vec{\vec{\eta}}_w \mathbf{h}_{\mathrm{loc}} \cdot \hat{\boldsymbol{\rho}})\hat{\boldsymbol{\rho}} - \vec{\vec{\eta}}_w \mathbf{h}_{\mathrm{loc}}]. \tag{24}$$

The second line of Eq. (24) follows from Eq. (8) and indicates that the scattered field is related to the incident field $\mathbf{h}_{\mathrm{loc}}$ by the external susceptibility tensor $\vec{\vec{\eta}}_w$.

Finally, by rearranging Eq. (18) in a form identical to Eq. (24), we find by identification the external susceptibility tensor of the wire,

$$\vec{\vec{\eta}}_w = \begin{pmatrix} \tilde{\eta} & -i\tilde{\eta}_t & 0 \\ i\tilde{\eta}_t & \tilde{\eta} & 0 \\ 0 & 0 & 0 \end{pmatrix}, \tag{25}$$

which is a gyrotropic tensor with diagonal and off-diagonal components expressed in terms of the renormalized permeability components $\tilde{\mu}$ and $\tilde{\mu}_t$ as

$$\tilde{\eta} = \frac{2(\tilde{\mu}^2 - \tilde{\mu}_t^2 - \mu_0^2)}{(\tilde{\mu}+\mu_0)^2 - \tilde{\mu}_t^2}, \quad \tilde{\eta}_t = \frac{4\mu_0\tilde{\mu}_t}{(\tilde{\mu}+\mu_0)^2 - \tilde{\mu}_t^2}. \tag{26}$$

Equations (25) and (26) constitute an important result of this work. They describe the complex and tensorial $k_w a$-dependent magnetization response of an axially magnetized metallic wire subjected to a transverse and uniform time-varying magnetic field. The treatment of electromagnetic retardation effects in the EQS regime is greatly simplified by our definitions for $\tilde{\mu}$ and $\tilde{\mu}_t$, which yield compact expressions for $\tilde{\eta}$ and $\tilde{\eta}_t$, identical in form to the results valid in the QS limit [see Eq. (28)]. The derivation of the external

susceptibility tensor $\overleftrightarrow{\eta}_w$ is also a key step of our homogenization procedure, which leads to the effective permeability tensor $\overleftrightarrow{\mu}_{\text{eff}}$, as derived in Sec. III.

The renormalized permeability components $\tilde{\mu}$ and $\tilde{\mu}_t$ incorporate, through the $k_w a$-dependent factor $G(k_w a)$, all electromagnetic propagation, attenuation, and size effects inside the wire. Consequently, the EQS response of the wire, characterized by the positions of the FMR and FMAR, as well as by the width, shape, and amplitude of the absorption curve, exhibits a nontrivial dependence on the product $k_w a$ and hence will generally not follow conventional FMR relations. In particular, the different contributions to the resonance linewidth of $\overleftrightarrow{\eta}_w$ are not easily distinguished in the EQS regime since $\tilde{\mu}$ and $\tilde{\mu}_t$ depend explicitly on the complex wave vector k_w. In ferromagnetic metals, k_w obeys a rather complicated dispersion relation that accounts for both the resonant behavior of the complex permeability $\overleftrightarrow{\mu}_w$ and the skin effect associated with the large conductivity σ_w. As a result, the observed linewidth reflects both the intrinsic magnetic losses due to Gilbert damping and those related to the eddy currents generated within the skin depth.

E. Validation of the model in the quasistatic and skin effect limits

In order to validate the general results presented in Sec. II D, we show how Eq. (26) allows us to recover various relations, which apply in the limits of weak and strong skin effect.

1. Quasistatic limit

In the QS approximation, uniform-mode magnetization oscillations are excited inside the wire and the fulfillment of Eq. (10) leads to $F(k_w a) \approx 1/2$ and $G(k_w a) \approx 1$. In such a case, we have $\tilde{\mu}=\mu$ and $\tilde{\mu}_t=\mu_t$ so that we recover the known QS size-independent expression for the external susceptibility tensor,[68]

$$\mathbf{m}_w = \overleftrightarrow{\eta}_w \mathbf{h}_{\text{loc}} = \begin{pmatrix} \eta & -i\eta_t & 0 \\ i\eta_t & \eta & 0 \\ 0 & 0 & 0 \end{pmatrix} \mathbf{h}_{\text{loc}} \tag{27}$$

with components

$$\eta = \frac{2(\mu^2 - \mu_t^2 - \mu_0^2)}{(\mu+\mu_0)^2 - \mu_t^2} = \frac{\omega_M(\omega_H^* + \omega_M/2)}{(\omega_H^* + \omega_M/2)^2 - \omega^2}, \tag{28a}$$

$$\eta_t = \frac{4\mu_0\mu_t}{(\mu+\mu_0)^2 - \mu_t^2} = \frac{\omega_M \omega}{(\omega_H^* + \omega_M/2)^2 - \omega^2}, \tag{28b}$$

which, in the low-damping limit $\alpha \ll 1$, have a pole at

$$\omega_r = \omega_H + \frac{\omega_M}{2}, \tag{29}$$

corresponding to the uniform-mode FMR frequency predicted by Kittel's formula for an axially magnetized infinite cylinder.[40] In the QS approximation, η and η_t retain the Lorentzian profile of μ and μ_t and have a linewidth determined solely by the intrinsic magnetic losses due to Gilbert damping.

An explicit tensorial relation between $\overleftrightarrow{\chi}_w$ and $\overleftrightarrow{\eta}_w$ can be established by working directly in the magnetostatic limit. In such a case, the field inside the wire can be expressed as[40]

$$\mathbf{h}_w = \mathbf{h}_{\text{loc}} - \overleftrightarrow{N}_w \mathbf{m}_w, \tag{30}$$

where the demagnetizing field $-\overleftrightarrow{N}_w \mathbf{m}_w$ is due to the shape of the wire and includes the demagnetizing tensor

$$\overleftrightarrow{N}_w = \begin{pmatrix} N_{\text{IP}}^w & 0 & 0 \\ 0 & N_{\text{IP}}^w & 0 \\ 0 & 0 & N_{\text{OP}}^w \end{pmatrix}, \tag{31}$$

with in-plane (IP) and out-of-plane (OP) demagnetizing factors N_{IP}^w and N_{OP}^w satisfying $2N_{\text{IP}}^w + N_{\text{OP}}^w = 1$.[70] Note that the IP and OP directions are defined in relation with the plane of a wire array, as considered in Sec. III.

Then, using Eqs. (4) and (27), we make the substitutions $\mathbf{h}_w = \overleftrightarrow{\chi}_w^{-1} \mathbf{m}_w$ and $\mathbf{h}_{\text{loc}} = \overleftrightarrow{\eta}_w^{-1} \mathbf{m}_w$ in Eq. (30) and recover the known QS tensorial relation between the intrinsic and external susceptibility tensors,[40]

$$\overleftrightarrow{\eta}_w^{-1} = \overleftrightarrow{\chi}_w^{-1} + \overleftrightarrow{N}_w. \tag{32}$$

Equation (32) indicates that the QS external response of the wire is size-independent and determined entirely by its intrinsic properties $\overleftrightarrow{\chi}_w$ and shape $\overleftrightarrow{N}_w$. It may be used to yield Eqs. (28a) and (28b) for the external susceptibility tensor components of a long wire with $N_{\text{IP}}^w = 1/2$ and $N_{\text{OP}}^w = 0$. Finally, we note that the QS regime correctly describes the FMR behavior expected for ferromagnetic-metallic nanowires with $a \leq 100$ nm.[31,35]

2. Skin effect limit

In the opposite limit of strong skin effect, the condition $|k_w| a \gg 1$ holds and the ratio of Bessel functions $J_1(k_w a)/J_0(k_w a)$ tends asymptotically to i. As a result, the renormalization factors $F(k_w a)$ and $G(k_w a)$ reduce to $i/k_w a$ so that their real and imaginary parts are both much smaller than 1. The renormalized permeability components are then well approximated by

$$\tilde{\mu} \approx \frac{i\mu(1-\beta^2)}{k_w a} = \frac{i\mu_\perp}{k_w a}, \tag{33a}$$

$$\tilde{\mu}_t \approx \frac{-\mu_t(1-\beta^2)}{(k_w a)^2} = -\frac{\mu_\perp \beta}{(k_w a)^2}, \tag{33b}$$

where $\mu_\perp = \mu(1-\beta^2)$ follows from Eq. (15). Equations (33a) and (33b) yield $\tilde{\mu}_t \approx (i\beta/k_w a)\tilde{\mu}$, from which we deduce that $\tilde{\mu} \gg \tilde{\mu}_t$. Hence, the inequality $\tilde{\eta} \gg \tilde{\eta}_t$ also holds so that the tensor $\overleftrightarrow{\tilde{\eta}}_w$ essentially reduces to the scalar quantity $\tilde{\eta}$. From Eq. (26), we find

$$\tilde{\eta} \approx \frac{2(\tilde{\mu}-\mu_0)}{(\tilde{\mu}+\mu_0)} \approx -2\left(1 - 2\frac{\tilde{\mu}}{\mu_0}\right), \tag{34}$$

where the condition $\tilde{\mu} \ll \mu_0$ was invoked to yield the right-hand side of Eq. (34). Equation (13) can be then used to

write Eq. (33a) in terms of δ_{w0}, which we substitute into Eq. (34) to yield

$$\tilde{\eta} \approx -2\left[1-(1+i)\frac{\delta_{w0}}{a}\sqrt{\frac{\mu_\perp}{\mu_0}}\right], \tag{35}$$

where the second term on the right-hand side is much smaller than 1. Note that for a nonmagnetic cylindrical conductor, we have $\mu_\perp=\mu_0$ and Eq. (35) simplifies to the known result $\tilde{\eta}\approx -2[1-(1+i)\delta_{w0}/a]\propto\omega^{-1/2}$ (e.g., see Ref. 41).

Alternatively, combining Eqs. (13) and (14) allows us to express $\tilde{\mu}$ in Eq. (33a) as $\tilde{\mu}=i\zeta_w/\omega a$. Inserting this result into Eq. (34), we recover the SE expression for $\tilde{\eta}$ derived in Ref. 42,

$$\tilde{\eta} \approx -2\left(1-\frac{2i}{k_m a}\frac{\zeta_w}{\zeta_m}\right). \tag{36}$$

Equation (36) shows that the magnetization response in the SE limit essentially follows that of the wire surface impedance ζ_w, which in our case can be written as

$$\zeta_w = \sqrt{\frac{\mu_\perp}{\epsilon_w}} = \sqrt{\frac{\mu_0}{\epsilon_w}}\left[\frac{(\omega_H^*+\omega_M)^2-\omega^2}{\omega_H^*(\omega_H^*+\omega_M)-\omega^2}\right]^{1/2} \tag{37}$$

and corresponds to an intrinsic, size-independent quantity. The SE limit applies well to the study of metallic microwires with radius on the order of 100 μm.[71] The pole and zero of ζ_w coincide with the FMR and FMAR frequencies of $\tilde{\eta}$, respectively. In the limit $\alpha \ll 1$, we find

$$\omega_r = \sqrt{\omega_H(\omega_H+\omega_M)}, \tag{38}$$

$$\omega_{\mathrm{ar}} = \omega_H+\omega_M. \tag{39}$$

In the SE limit, the FMR frequency ω_r thus corresponds to that of parallel resonance in metals in which the wave vector is perpendicular to the direction of steady magnetization.[40]

Equation (36) also exhibits the FMAR phenomenon at ω_{ar}, where the real part of the surface impedance ζ_w reaches a minimum, corresponding to a vanishing average magnetic induction within the wire. Following Faraday's and Ohm's laws, the induced eddy currents and corresponding losses will then be strongly reduced, leading to a significant enhancement of the skin depth and to a minimum in the absorption, governed by $\mathrm{Im}[\tilde{\eta}]$. Note that the FMAR is not observed in the QS limit since in this case the skin depth is always larger than the wire radius. Consequently, eddy-current losses remain negligible in all cases and the absorption curve does not exhibit a local minimum.

For a perfectly conducting wire ($\sigma_w\to\infty$), the surface impedance ζ_w tends to 0 and the SE external susceptibility further reduces to $\tilde{\eta}=-2$. In this case, a conducting wire placed in a high-frequency magnetic field behaves as a perfectly diamagnetic (i.e., superconducting) body with a static permeability of zero subjected to a steady magnetic field.[41] Indeed, substituting $\mu=0$ (along with $\mu_t=0$) into Eq. (28a) yields $\eta=-2$ for the QS external susceptibility of a superconducting wire placed in a transverse magnetic field, which is identical to the perfectly conducting SE limit of Eq. (36).

TABLE I. Definition of the susceptibility tensors and associated constitutive relations.

Susceptibility tensor	Constitutive relation
Intrinsic $\overleftrightarrow{\chi}_w$	$\mathbf{m}_w=\overleftrightarrow{\chi}_w\mathbf{h}_w$
External $\overleftrightarrow{\eta}_w$	$\langle\mathbf{m}_w\rangle=\overleftrightarrow{\eta}_w\mathbf{h}_{\mathrm{loc}}$
Effective $\overleftrightarrow{\chi}_{\mathrm{eff}}$	$\langle\mathbf{m}\rangle=\overleftrightarrow{\chi}_{\mathrm{eff}}\langle\mathbf{h}\rangle$
Effective external $\overleftrightarrow{\eta}_{\mathrm{eff}}$	$\langle\mathbf{m}\rangle=\overleftrightarrow{\eta}_{\mathrm{eff}}\mathbf{h}_{\mathrm{ext}}$

In summary, the QS and SE limits of the general EQS response are characterized by size-independent FMR parameters. In particular, while the linewidth of the external susceptibility is governed by the Gilbert parameter α in the QS case (smaller diameters), it is essentially related to the real part of the surface impedance ζ_w in the SE limit (larger diameters). Between these two limiting cases, the general EQS expressions must be used and lead to size-dependent FMR properties.

III. DYNAMIC RESPONSE OF AN ARRAY OF FERROMAGNETIC WIRES

In this section, we present our derivation of the EQS effective permeability tensor $\overleftrightarrow{\mu}_{\mathrm{eff}}$ of arrays of axially magnetized ferromagnetic wires, incorporating both the gyromagnetic and $k_w a$-dependent responses of the individual wires. Our multiscale theoretical approach has so far considered two hierarchical levels (i.e., intrinsic and external) to describe the response of a single wire. Each level was associated with a susceptibility tensor connecting the dynamic magnetization of the wire to a specific magnetic field. The intrinsic susceptibility $\overleftrightarrow{\chi}_w$ depends on the wire composition and accounts for the response of the wire magnetization to the internal field [Eq. (4)]. The intrinsic response was then incorporated into the scattering problem to derive the EQS external susceptibility tensor $\overleftrightarrow{\eta}_w$ of an axially magnetized metallic wire of given size and shape, in order to relate the average magnetization response to the magnetic field of the incident wave [Eq. (8)].

In the following, we extend the distinction between intrinsic and external responses to an array of wires by introducing, in addition to the usual Maxwell-Garnett effective susceptibility tensor $\overleftrightarrow{\chi}_{\mathrm{eff}}$ [Eq. (53)], the effective external susceptibility tensor $\overleftrightarrow{\eta}_{\mathrm{eff}}$ [Eq. (58)]. The former will be derived in this section and represents an intrinsic bulk property relating the average magnetization and field inside the homogenized wire array, whereas the latter will be considered in Sec. IV to describe uniform-mode magnetization oscillations in finite-size arrays. The susceptibility tensors and corresponding constitutive relations related to the four hierarchical levels considered in this paper are summarized in Table I.

A. Preliminary considerations

The interaction of electromagnetic waves with heterogeneous materials is commonly studied within the framework of effective-medium theories. When the length of the wave propagating within the composite material is much larger

than the characteristic size a and separation D of the inclusions, the medium can be treated as homogeneous and be characterized by effective permeability and permittivity tensors relating the average fields and inductions inside the material,

$$\langle \mathbf{b} \rangle = \overleftrightarrow{\mu}_{\text{eff}} \langle \mathbf{h} \rangle, \tag{40}$$

$$\langle \mathbf{d} \rangle = \overleftrightarrow{\epsilon}_{\text{eff}} \langle \mathbf{e} \rangle, \tag{41}$$

where angular brackets denote appropriately defined spatial averages of alternating field quantities.

The tensors $\overleftrightarrow{\mu}_{\text{eff}}$ and $\overleftrightarrow{\epsilon}_{\text{eff}}$ must be interpreted as intrinsic properties of the composite material, which play the same roles as those of $\overleftrightarrow{\mu}_w$ and $\overleftrightarrow{\epsilon}_w$ in the context of homogeneous media. Inside the composite, the propagation of a plane wave of the form $e^{i(\mathbf{k}_{\text{eff}} \cdot \mathbf{r} - \omega t)}$ is then governed by macroscopic Maxwell's equations, expressed in terms of $\overleftrightarrow{\mu}_{\text{eff}}$ and $\overleftrightarrow{\epsilon}_{\text{eff}}$ as

$$\mathbf{k}_{\text{eff}} \times \langle \mathbf{h} \rangle = -\omega \overleftrightarrow{\epsilon}_{\text{eff}} \langle \mathbf{e} \rangle, \tag{42a}$$

$$\mathbf{k}_{\text{eff}} \times \langle \mathbf{e} \rangle = \omega \overleftrightarrow{\mu}_{\text{eff}} \langle \mathbf{h} \rangle, \tag{42b}$$

where $\mathbf{k}_{\text{eff}}$ is the effective wave vector. Note that our definition for $\overleftrightarrow{\epsilon}_{\text{eff}}$ includes the effective conductivity tensor of the composite material. Combining the two Maxwell's equations leads to the dispersion relation $\omega(\mathbf{k}_{\text{eff}})$ of the composite material, the solutions of which are the wave vectors of the propagating waves, expressed in terms of the components of the effective permeability and permittivity tensors. These may then be inserted into the appropriate boundary conditions to relate the fields $\mathbf{e}_{\text{ext}}$ and $\mathbf{h}_{\text{ext}}$ of an incident wave to the fields $\langle \mathbf{e} \rangle$ and $\langle \mathbf{h} \rangle$ inside the composite and to extract the electromagnetic parameters of interest.

In the following, we derive analytical expressions for the diagonal and off-diagonal components of $\overleftrightarrow{\mu}_{\text{eff}}$ in the limits $|k_{\text{eff}}|D \ll 1$ and $|k_{\text{eff}}|a \ll 1$. The main result is expressed in terms of the EQS external susceptibility tensor $\overleftrightarrow{\eta}_w$ of the individual wires obtained in Sec. II, therefore incorporating both their gyromagnetic and $k_w a$-dependent responses. A similar derivation for the effective permittivity $\overleftrightarrow{\epsilon}_{\text{eff}}$ of arrays of ferromagnetic wires will be presented elsewhere.

B. Effective permeability tensor

Consider an array of axially magnetized ferromagnetic-metallic wires of diameter $d=2a$, length $L \gg d$, and interwire distance D, embedded in the pores of a dielectric thin-film matrix of permittivity ϵ_m, permeability $\mu_m=\mu_0$, thickness L, and lateral extent $2R$. The wires occupy a volume fraction $f=f_0(\pi a^2/D^2)$ of the array, where f_0 is a constant depending on the spatial arrangement of the pores. To simplify the calculations and with no loss of generality, we henceforth assume that $f_0=1$, corresponding to a square network of wires. The magnetic response of the individual wires is accounted for by the external susceptibility tensor $\overleftrightarrow{\eta}_w$ given in Eq. (25). The axis of the wires and the plane of the array correspond to the OP and IP directions, respectively. Schematic representations of the array and of the unit cell of size D containing a wire of radius a at its center are shown in Figs. 2(a) and 2(b), respectively.

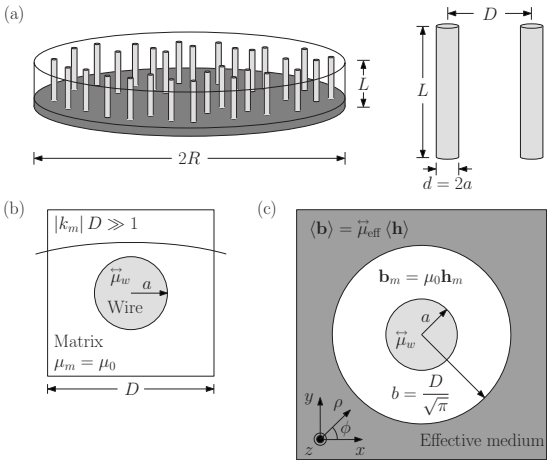

FIG. 2. (a) Schematic representation of the ferromagnetic wire array and definition of the relevant geometrical parameters. (b) Definition of the square unit cell of side D containing a wire of radius a at its center. (c) Definition of the equivalent circular unit cell of radius $b=D/\sqrt{\pi}$ embedded in the effective medium and introduced to derive the effective permeability tensor $\overleftrightarrow{\mu}_{\text{eff}}$. Note that the origin of the coordinate systems in (c) coincides with the center of the wire.

We wish to derive $\overleftrightarrow{\mu}_{\text{eff}}$ in the general electromagnetic regime, for which wave propagation is allowed inside the array and no restriction is imposed on the value of $|k_{\text{eff}}|R$. First, we suppose that the square unit cell in Fig. 2(b) may be replaced by the equivalent circular unit cell shown in Fig. 2(c), consisting of a wire of radius a coated by a layer of matrix material of outer radius $b=D/\sqrt{\pi}$ so that the volume fraction $f=a^2/b^2=\pi a^2/D^2$ remains unchanged. The wire axis defines the z axis of both a rectangular (x,y,z) and a cylindrical (ρ,ϕ,z) coordinate systems. Further, we assume that this equivalent unit cell is immersed into an effective medium defined by the constitutive relation $\langle \mathbf{b} \rangle = \overleftrightarrow{\mu}_{\text{eff}} \langle \mathbf{h} \rangle$ [Eq. (40)], from which we aim to determine $\overleftrightarrow{\mu}_{\text{eff}}$. Introducing the circular unit cell allows us to simplify the analytical calculations but requires that its field distribution does not differ significantly from that of the square cell. This approach based on an equivalent unit cell has been followed in recent studies to yield the *scalar* effective EQS response of various magneto-dielectric composites[72] and photonic crystals[10,73] within the coherent-potential approximation.[74]

Here, an expression for the *gyrotropic* tensor $\overleftrightarrow{\mu}_{\text{eff}}$ in terms of $\overleftrightarrow{\eta}_w$ will be obtained. Our homogenization procedure is based on the satisfaction of the appropriate boundary conditions on the magnetic field and induction at the interface $\rho=b$ between the equivalent unit cell and the effective medium. Considering the cylindrical symmetry of the problem, this implies that the conditions

$$\langle \mathbf{h} \rangle \cdot \hat{\boldsymbol{\phi}} = \mathbf{h}_m \cdot \hat{\boldsymbol{\phi}}, \tag{43a}$$

$$\langle \mathbf{b} \rangle \cdot \hat{\boldsymbol{\rho}} = \mathbf{b}_m \cdot \hat{\boldsymbol{\rho}} \tag{43b}$$

hold at $\rho=b$, where $\mathbf{h}_m$ and $\mathbf{b}_m$ are the field and induction in the outer matrix layer of the equivalent unit cell, respectively.

Our procedure will consist in applying Eqs. (43a) and (43b) at $\rho=b$ and for different values of ϕ, in order to express $\langle \mathbf{h} \rangle$ and $\langle \mathbf{b} \rangle$ in terms of the local field $\mathbf{h}_{\mathrm{loc}}$ acting on the wire at the center of the unit cell [Eq. (17)]. The resulting expressions for $\langle \mathbf{h} \rangle$ and $\langle \mathbf{b} \rangle$ will then be substituted in Eq. (40) to yield $\vec{\tilde{\mu}}_{\mathrm{eff}}$.

The first step of the homogenization problem thus requires one to relate the fields $\mathbf{h}_m$ and $\mathbf{b}_m$ in the matrix to the local field $\mathbf{h}_{\mathrm{loc}}$. In the limit $|k_m|D \ll 1$, we may substitute Eqs. (17) and (24) into Eq. (16) to yield the magnetic field in the outer layer of matrix material

$$\mathbf{h}_m = \mathbf{h}_{\mathrm{loc}} + \frac{a^2}{2\rho^2}[2(\vec{\tilde{\eta}}_w \mathbf{h}_{\mathrm{loc}} \cdot \hat{\boldsymbol{\rho}})\hat{\boldsymbol{\rho}} - \vec{\tilde{\eta}}_w \mathbf{h}_{\mathrm{loc}}]$$

$$= \mathbf{h}_{\mathrm{loc}} + \frac{a^2}{2\rho^2}[2(\hat{\boldsymbol{\rho}} \circ \hat{\boldsymbol{\rho}}) - \vec{I}]\vec{\tilde{\eta}}_w \mathbf{h}_{\mathrm{loc}}, \tag{44}$$

where the components of $\vec{\tilde{\eta}}_w$ are given by Eq. (26) and $\hat{\boldsymbol{\rho}} \circ \hat{\boldsymbol{\rho}}$ corresponds to the dyadic product of $\hat{\boldsymbol{\rho}} = \cos\phi \hat{\mathbf{x}} + \sin\phi \hat{\mathbf{y}}$ with itself. This leads to

$$[2(\hat{\boldsymbol{\rho}} \circ \hat{\boldsymbol{\rho}}) - \vec{I}] = \begin{pmatrix} \cos 2\phi & \sin 2\phi \\ \sin 2\phi & -\cos 2\phi \end{pmatrix}, \tag{45}$$

which can be substituted into Eq. (44) to yield explicit expressions for the x and y components of $\mathbf{h}_m = h_{m,x}(\rho,\phi)\hat{\mathbf{x}} + h_{m,y}(\rho,\phi)\hat{\mathbf{y}}$ in terms of $\mathbf{h}_{\mathrm{loc}} = -h_{\mathrm{loc}}\hat{\mathbf{y}}$. The magnetic induction in the matrix follows directly from $\mathbf{b}_m = \mu_0 \mathbf{h}_m$.

Then, we relate $\mathbf{h}_m$ and $\mathbf{b}_m$ to the average fields $\langle \mathbf{h} \rangle$ and $\langle \mathbf{b} \rangle$ by satisfying the boundary conditions for the continuity of the tangential component of the magnetic field [Eq. (43a)] and the normal component of the magnetic induction [Eq. (43b)]. These requirements imply that the y component of the magnetic field and the x component of the magnetic induction are continuous at $(\rho=b,\ \phi=0,\pi)$, leading to

$$\langle h_y \rangle = h_{m,y} = -\left(1 - \frac{f\tilde{\eta}}{2}\right) h_{\mathrm{loc}}, \tag{46a}$$

$$\langle b_x \rangle = b_{m,x} = i\mu_0 \left(\frac{f\tilde{\eta}_t}{2}\right) h_{\mathrm{loc}}. \tag{46b}$$

Likewise, at $(\rho=b,\ \phi=\pm\pi/2)$, the x component of the magnetic field and the y component of the magnetic induction are continuous, which yields

$$\langle h_x \rangle = h_{m,x} = -i\left(\frac{f\tilde{\eta}_t}{2}\right) h_{\mathrm{loc}}, \tag{47a}$$

$$\langle b_y \rangle = b_{m,y} = -\mu_0 \left(1 + \frac{f\tilde{\eta}}{2}\right) h_{\mathrm{loc}}. \tag{47b}$$

We must emphasize that the volume fraction $f=a^2/b^2$ is introduced into the boundary conditions by evaluating the term a^2/ρ^2 in $\mathbf{h}_m$ and $\mathbf{b}_m$ at $\rho=b$ [see Eq. (44)].

Next, we combine Eqs. (46) and (47) to yield tensorial expressions relating the average field $\langle \mathbf{h} \rangle$ and induction $\langle \mathbf{b} \rangle$ to the local field $\mathbf{h}_{\mathrm{loc}}$ exciting the individual wires in the array,

$$\langle \mathbf{h} \rangle = [\vec{I} - f\vec{N}_w \vec{\tilde{\eta}}_w]\mathbf{h}_{\mathrm{loc}}, \tag{48}$$

$$\langle \mathbf{b} \rangle = \mu_0[\vec{I} + f(\vec{I} - \vec{N}_w)\vec{\tilde{\eta}}_w]\mathbf{h}_{\mathrm{loc}}, \tag{49}$$

where $\vec{N}_w$ is given by Eq. (31) and has in-plane components $N_{\mathrm{IP}}^w = 1/2$. Finally, substituting Eq. (48) into Eq. (40) and comparing with Eq. (49) yield a Maxwell-Garnett-type expression for the EQS effective permeability tensor

$$\frac{\vec{\tilde{\mu}}_{\mathrm{eff}}}{\mu_0} = \vec{I} + f[\vec{\tilde{\eta}}_w^{-1} - f\vec{N}_w]^{-1}. \tag{50}$$

Straightforward calculations demonstrate that $\vec{\tilde{\mu}}_{\mathrm{eff}}$ retains the gyrotropic nature of $\vec{\tilde{\eta}}_w$ and can be put in the form

$$\vec{\tilde{\mu}}_{\mathrm{eff}} = \mu_0(\vec{I} + \vec{\chi}_{\mathrm{eff}}) = \begin{pmatrix} \tilde{\mu}_{\mathrm{eff}} & -i\tilde{\mu}_{\mathrm{eff},t} & 0 \\ i\tilde{\mu}_{\mathrm{eff},t} & \tilde{\mu}_{\mathrm{eff}} & 0 \\ 0 & 0 & \mu_0 \end{pmatrix}, \tag{51}$$

with diagonal and off-diagonal components

$$\frac{\tilde{\mu}_{\mathrm{eff}}}{\mu_0} = 1 + 2f\left[\frac{2\tilde{\eta} - f(\tilde{\eta}^2 - \tilde{\eta}_t^2)}{(f\tilde{\eta} - 2)^2 - (f\tilde{\eta}_t)^2}\right], \tag{52a}$$

$$\frac{\tilde{\mu}_{\mathrm{eff},t}}{\mu_0} = \frac{4f\tilde{\eta}_t}{(f\tilde{\eta} - 2)^2 - (f\tilde{\eta}_t)^2}. \tag{52b}$$

In Eq. (51), we introduced the effective susceptibility tensor $\vec{\chi}_{\mathrm{eff}}$, which satisfies

$$\langle \mathbf{m} \rangle = \vec{\chi}_{\mathrm{eff}} \langle \mathbf{h} \rangle = f[\vec{\tilde{\eta}}_w^{-1} - f\vec{N}_w]^{-1} \langle \mathbf{h} \rangle \tag{53}$$

and thus relates the average dynamic magnetic field $\langle \mathbf{h} \rangle$ to the average dynamic magnetization of the array $\langle \mathbf{m} \rangle = f\langle \mathbf{m}_w \rangle$, which is equal to the volume fraction times the average magnetization of the individual wires.

The effective gyrotropic permeability tensor $\vec{\tilde{\mu}}_{\mathrm{eff}}$ accounts for the EQS external susceptibility tensor $\vec{\tilde{\eta}}_w$ of the wires, including magnetic damping and electromagnetic retardation, as well as their shape $\vec{N}_w$ and volume fraction f. The response also depends on the static magnetic field inside the wires, which in an array has contributions from both the external field H_{ext0} and dipolar interactions.[35]

C. Recovery of various expressions for the effective permeability as particular cases

Our general result for $\vec{\tilde{\mu}}_{\mathrm{eff}}$ allows us to recover several limiting results as particular cases. In Ref. 10, a model describing the EQS effective electromagnetic response of a composite material consisting of insulating ferrimagnetic rods described by the gyromagnetic permeability tensor of Eqs. (3) and (5) was developed and lead to an effective isotropic permeability, which can be recovered from our Eq. (52) as follows:

$$\tilde{\mu}_{\mathrm{eff}\perp} = \frac{\tilde{\mu}_{\mathrm{eff}}^2 - \tilde{\mu}_{\mathrm{eff},t}^2}{\tilde{\mu}_{\mathrm{eff}}} = \mu_0 \frac{(f\tilde{\eta} + 2)^2 - (f\tilde{\eta}_t)^2}{4 - f^2(\tilde{\eta}^2 - \tilde{\eta}_t^2)}. \tag{54}$$

Direct calculations show that Eq. (54) corresponds exactly to Eq. (13b) of Ref. 10. The effective permeability $\tilde{\mu}_{\mathrm{eff}\perp}$ con-

stitutes a particular combination of the components of $\vec{\vec{\mu}}_{\text{eff}}$, which characterizes wave propagation in the plane of an *unbounded* array of axially magnetized wires. However, in the context of guided waves propagating in *bounded* structures[75,76] or FMR cavity measurements in finite-size arrays (treated in Sec. IV), one must consider the full gyrotropic form of $\vec{\vec{\mu}}_{\text{eff}}$ in order to yield a complete description of the magnetic response.

For wires with an isotropic permeability μ, the external susceptibility $\tilde{\eta}=2(\tilde{\mu}-\mu_0)/(\tilde{\mu}+\mu_0)$ reduces to a scalar quantity with $\tilde{\mu}=\mu G(k_w a)$. Then, Eq. (50) simplifies to

$$\frac{\tilde{\mu}_{\text{eff}}}{\mu_0}=\frac{2+f\tilde{\eta}}{2-f\tilde{\eta}}=\frac{\tilde{\mu}(1+f)+\mu_0(1-f)}{\tilde{\mu}(1-f)+\mu_0(1+f)} \tag{55}$$

and one recovers the EQS effective permeability of an array of isotropic wires excited by a transverse dynamic magnetic field,[55,72,77,78] which was initially established in Ref. 50.

In the QS limit, the components of $\vec{\vec{\eta}}_w$ are given by Eqs. (28a) and (28b). Hence, using Eqs. (3) and (32), allows us to recover the known expression[8,44,47]

$$\frac{\vec{\vec{\mu}}_{\text{eff}}}{\mu_0}=\vec{\vec{I}}+f\left[\left(\frac{\vec{\vec{\mu}}_w}{\mu_0}-\vec{\vec{I}}\right)^{-1}+(1-f)\vec{\vec{N}}_w\right]^{-1}. \tag{56}$$

Finally, for isotropic wires in the QS limit, we find that $\tilde{\eta}=\eta=2(\mu-\mu_0)/(\mu+\mu_0)$ and $\tilde{\mu}_{\text{eff}}=\mu_{\text{eff}}$ so that Eq. (50) reduces to

$$\frac{\mu_{\text{eff}}-\mu_0}{\mu_{\text{eff}}+\mu_0}=f\frac{\mu-\mu_0}{\mu+\mu_0}=\frac{f\eta}{2} \tag{57}$$

and corresponds to the conventional forms of the Maxwell-Garnett and Clausius-Mossotti formulas.

IV. EFFECTIVE EXTERNAL RESPONSE AND DIPOLAR INTERACTIONS

Homogenization procedures leading to effective constitutive parameters, such as described in Sec. III, assume that the composite material is unbounded. The effect of surface poles in finite-size samples is thus not yet accounted for. In the most general situation, the effective permeability tensor $\vec{\vec{\mu}}_{\text{eff}}$ defined in Eqs. (50)–(52) would enter the macroscopic Maxwell's equations to describe the propagation of electromagnetic waves of the form $e^{i(\mathbf{k}_{\text{eff}}\mathbf{r}-\omega t)}$ inside the wire array, subjected to the appropriate boundary conditions. Following up on our multiscale approach, we could further define an *effective external* susceptibility tensor $\vec{\vec{\eta}}_{\text{eff}}$, which would describe the response of finite-size samples to an external (i.e., experimentally controlled) uniform dynamic magnetic field. Indeed, in such a case, the treatment of the general electromagnetic problem simplifies considerably since the condition $|k_{\text{eff}}|R\ll 1$ holds and uniform oscillations of $\langle\mathbf{m}\rangle$ are excited in the composite. These requirements are usually fulfilled in uniform-mode FMR measurements involving sufficiently small wire arrays. Such experiments have proved extremely useful in studying the effect of the interwire dipolar interactions on the microwave response of arrays of ferromagnetic-metallic nanowires.[31–35]

In this section, we demonstrate how the measured FMR response can be properly characterized by the effective external susceptibility tensor $\vec{\vec{\eta}}_{\text{eff}}$, along with an effective demagnetizing tensor. We also clarify the relations between demagnetizing tensors used in different FMR theories and show how they arise in our formalism based on $\vec{\vec{\eta}}_{\text{eff}}$.

A. Effective external susceptibility tensor

We consider the wire array of diameter $2R$, thickness $L\ll R$, and effective susceptibility tensor $\vec{\vec{\chi}}_{\text{eff}}$, as shown in Fig. 2(a). The array is subjected to a uniform time-varying field $\mathbf{h}_{\text{ext}}$, which excites uniform oscillations of the magnetization $\langle\mathbf{m}\rangle$ according to the constitutive relation

$$\langle\mathbf{m}\rangle=\vec{\vec{\eta}}_{\text{eff}}\mathbf{h}_{\text{ext}}=\begin{pmatrix}\tilde{\eta}_{\text{eff}} & -i\tilde{\eta}_{\text{eff},t} & 0\\ i\tilde{\eta}_{\text{eff},t} & \tilde{\eta}_{\text{eff}} & 0\\ 0 & 0 & 0\end{pmatrix}\mathbf{h}_{\text{ext}}, \tag{58}$$

where the effective external susceptibility $\vec{\vec{\eta}}_{\text{eff}}$ is a gyrotropic tensor with diagonal and off-diagonal components $\tilde{\eta}_{\text{eff}}$ and $\tilde{\eta}_{\text{eff},t}$, which connects the dynamic magnetization of the array to the external field. We wish to establish a relation between the effective external susceptibility $\vec{\vec{\eta}}_{\text{eff}}$ and the effective susceptibility $\vec{\vec{\chi}}_{\text{eff}}$ derived in Sec. III. To do so, let us introduce the effective demagnetizing tensor $\vec{\vec{N}}_{\text{eff}}$, such that Eq. (30) can be generalized to the case of composite materials as

$$\langle\mathbf{h}\rangle=\mathbf{h}_{\text{ext}}-\vec{\vec{N}}_{\text{eff}}\langle\mathbf{m}\rangle. \tag{59}$$

This provides a link between the uniform time-varying field $\langle\mathbf{h}\rangle$ inside the array and the external field $\mathbf{h}_{\text{ext}}$. The tensor $\vec{\vec{N}}_{\text{eff}}$ accounts for surface poles at the boundaries of the finite-size array and thus can be interpreted as a shape demagnetizing tensor for the homogenized composite material. In Sec. IV B, we will use dipolar interactions to derive an explicit expression for $\vec{\vec{N}}_{\text{eff}}$ and we will show how it is related to the shape demagnetizing tensor of a thin disk of radius R and thickness L. For the time being, let us just assume that $\vec{\vec{N}}_{\text{eff}}$ exists and fulfills Eq. (59). Then, in a manner similar to the derivation of Eq. (32), we use Eqs. (53) and (58) to make the substitutions $\langle\mathbf{h}\rangle=\vec{\vec{\chi}}_{\text{eff}}^{-1}\langle\mathbf{m}\rangle$ and $\mathbf{h}_{\text{ext}}=\vec{\vec{\eta}}_{\text{eff}}^{-1}\langle\mathbf{m}\rangle$ into Eq. (59), resulting in

$$\vec{\vec{\eta}}_{\text{eff}}^{-1}=\vec{\vec{\chi}}_{\text{eff}}^{-1}+\vec{\vec{N}}_{\text{eff}}. \tag{60}$$

This effective external susceptibility tensor constitutes the relevant response function in uniform-mode FMR experiments. Equation (60) emphasizes the importance to distinguish between $\vec{\vec{\chi}}_{\text{eff}}$ and $\vec{\vec{\eta}}_{\text{eff}}$. The former corresponds to the magnetization response of the composite to the average internal field, regardless of the size and shape of the sample, and enters the macroscopic Maxwell's equations to describe propagation of electromagnetic waves within the homogenized material. The latter represents the response to an external field in the limit $|k_{\text{eff}}|R\ll 1$ and depends on the shape of the specimen through the tensor $\vec{\vec{N}}_{\text{eff}}$. In particular, it is the pole of $\vec{\vec{\eta}}_{\text{eff}}$, rather than that of $\vec{\vec{\chi}}_{\text{eff}}$, that determines the FMR parameters measured in microwave cavity experiments.

B. Dipolar interactions

An expression for $\overleftrightarrow{N}_{\text{eff}}$ can be obtained by linking the FMR response of the array of interacting wires to that of a single wire, calculated in Sec. II. This requires an expression for $\overleftrightarrow{\eta}_{\text{eff}}$ in terms of $\overleftrightarrow{\eta}_w$, which we establish by combining Eqs. (53) and (60) to yield

$$\left(\frac{\overleftrightarrow{\eta}_{\text{eff}}}{f}\right)^{-1} = \overleftrightarrow{\eta}_w^{-1} + f(\overleftrightarrow{N}_{\text{eff}} - \overleftrightarrow{N}_w), \tag{61}$$

where the term $f(\overleftrightarrow{N}_{\text{eff}}-\overleftrightarrow{N}_w)$ corresponds to the dynamic dipolar interactions between the wires, as demonstrated below. Since we are in the limit $|k_{\text{eff}}|R \ll 1$, the local field $\mathbf{h}_{\text{loc}}$ acting on a given wire in the array is the sum the external field $\mathbf{h}_{\text{ext}}$ and the dipolar interaction field $\mathbf{h}_{\text{int}}$ created by all the other wires. It can be written as

$$\mathbf{h}_{\text{loc}} = \mathbf{h}_{\text{ext}} + \mathbf{h}_{\text{int}} = \mathbf{h}_{\text{ext}} - \overleftrightarrow{N}_{\text{int}}\langle \mathbf{m}_w \rangle, \tag{62}$$

where $\overleftrightarrow{N}_{\text{int}}$ is the interaction tensor used in Ref. 35 to model the QS angle-dependent FMR response of nanowire arrays, including both intrawire and interwire dipolar interactions. The out-of-plane (axial) component of $\overleftrightarrow{N}_{\text{int}}$ is given by

$$N_{\text{OP}}^{\text{int}} = f\sum_{n=1}^{\infty} \frac{ns}{(n^2+s^2)^{3/2}}, \tag{63}$$

where $s=L/2D$ is a normalized length parameter. The sum in Eq. (63) depends on geometrical parameters only and tends asymptotically to unity in the monopolar regime, defined by the condition $L \gg D$. In such a case, $N_{\text{OP}}^{\text{int}}$ reduces to f and the two in-plane components $N_{\text{IP}}^{\text{int}}$ tends to $-f/2$ since the interaction tensor has a trace of zero.[35,79]

Using Eqs. (8) and (58) to replace $\mathbf{h}_{\text{loc}}=\overleftrightarrow{\eta}_w^{-1}\langle \mathbf{m}_w \rangle$ and $\mathbf{h}_{\text{ext}}=\overleftrightarrow{\eta}_{\text{eff}}^{-1}\langle \mathbf{m} \rangle = f\overleftrightarrow{\eta}_{\text{eff}}^{-1}\langle \mathbf{m}_w \rangle$ in Eq. (62), we obtain

$$\left(\frac{\overleftrightarrow{\eta}_{\text{eff}}}{f}\right)^{-1} = \overleftrightarrow{\eta}_w^{-1} + \overleftrightarrow{N}_{\text{int}}. \tag{64}$$

Equation (64) shows the effect of interwire dipolar interactions in modifying the FMR response of an array of interacting wires. Neglecting interwire interactions is equivalent to setting $\overleftrightarrow{N}_{\text{int}}=0$ in Eq. (64), which leads to the dilute response $\overleftrightarrow{\eta}_{\text{eff}}=f\overleftrightarrow{\eta}_w$. In such a case, one would conclude that the FMR frequency of the composite material is the same as that of the individual inclusions. This is correct for dilute magnetic composites.[45] However, for relatively dense composite materials,[35] the interwire dipolar interactions will significantly modify the FMR response and cannot be neglected.

Now, comparing Eqs. (61) and (64) leads to a definition for the effective demagnetizing tensor of the array

$$\overleftrightarrow{N}_{\text{eff}} = \overleftrightarrow{N}_w + f^{-1}\overleftrightarrow{N}_{\text{int}} \tag{65}$$

in terms of the geometry-dependent internal tensors $\overleftrightarrow{N}_w$ and $\overleftrightarrow{N}_{\text{int}}$. However, the form of Eqs. (59) and (60) suggests that $\overleftrightarrow{N}_{\text{eff}}$ also represents the shape demagnetizing tensor of the wire array. Hence, it is relevant to examine how Eq. (65) for $\overleftrightarrow{N}_{\text{eff}}$ compares with the demagnetizing tensor $\overleftrightarrow{N}_d$ of a homogeneously magnetized disk with the shape of the wire array. The OP demagnetizing factor N_{OP}^d at the center of a circular disk of radius R and thickness L is[80]

$$N_{\text{OP}}^d = 1 - \frac{l}{(1+l^2)^{1/2}}, \tag{66}$$

where $l=L/2R$ is the aspect ratio of the disk. The IP components N_{IP}^d can be obtained from the trace relation $2N_{\text{IP}}^d + N_{\text{OP}}^d = 1$. Further, for a disk of infinite lateral extent, l tends to 0, leading to $N_{\text{OP}}^d \approx 1$ and $N_{\text{IP}}^d \approx 0$, as expected for an infinitely thin circular plate.[40]

Let us now demonstrate that for long wires ($L \gg d$) in the monopolar regime ($L \gg D$), Eq. (65) reduces simply to Eq. (66), that is, $\overleftrightarrow{N}_w + f^{-1}\overleftrightarrow{N}_{\text{int}}$ coincides with the shape demagnetizing tensor $\overleftrightarrow{N}_d$ of a thin disk with uniform average magnetization $\langle \mathbf{m} \rangle$. First, for long wires, the shape demagnetizing tensor $\overleftrightarrow{N}_w$ has IP and OP components N_{IP}^w and N_{OP}^w equal to 1/2 and 0, respectively. Then, for a finite wire array, the OP component of the interaction tensor can be written as Eq. (63) for the infinite case, minus the contribution from the wires lying outside the finite array of radius R. At the center of the array, this yields

$$N_{\text{OP}}^{\text{int}} = \sum_{n=1}^{\infty} \frac{fns}{(n^2+s^2)^{3/2}} - \sum_{n=n_{\max}}^{\infty} \frac{fns}{(n^2+s^2)^{3/2}}, \tag{67}$$

where $n_{\max}=R/D$ is the number of wires on a line going from the center to the edge of the array. In the monopolar regime, the first term reduces to the porosity f. Further, we assume that the wires beyond R are located sufficiently far from the center of the array to be treated as continuous magnetization distribution. Then, we can transform the second sum over n into an integral and obtain

$$N_{\text{OP}}^{\text{int}} = f\left[1 - \int_{n_{\max}}^{\infty} \frac{ns}{(n^2+s^2)^{3/2}} dn\right] = f\left[1 - \frac{l}{(1+l^2)^{1/2}}\right], \tag{68}$$

where $l=s/n_{\max}=L/2R$. For long wires with $N_{\text{OP}}^w=0$, it follows that

$$N_{\text{OP}}^{\text{eff}} = N_{\text{OP}}^w + f^{-1}N_{\text{OP}}^{\text{int}} = 1 - \frac{l}{(1+l^2)^{1/2}}, \tag{69}$$

which, as expected, coincides with Eq. (66) for the OP demagnetizing factor at the center of a thin disk of radius R and thickness L. The relation is also satisfied for the IP components $N_{\text{IP}}^{\text{eff}}$, which follow from the trace relations $2N_{\text{IP}}^w + N_{\text{OP}}^w = 1$ and $2N_{\text{IP}}^{\text{int}} + N_{\text{OP}}^{\text{int}} = 0$. Likewise, for an infinite array, Eq. (63) yields $N_{\text{OP}}^{\text{int}}=f$ and thus $N_{\text{IP}}^{\text{int}}=-f/2$. This leads to $N_{\text{OP}}^{\text{eff}}=1$ and $N_{\text{IP}}^{\text{eff}}=0$, which also coincide with the shape demagnetizing factors N_{OP}^d and N_{IP}^d of an infinite thin disk.

Hence, in the limits $L \gg d$ and $L \gg D$, Eq. (69) indicates that our more general approach, which includes dipolar interactions and leads to the effective demagnetizing tensor $\overleftrightarrow{N}_{\text{eff}}$ of Eq. (65), indeed reduces to a simple macroscopic

TABLE II. Intrinsic properties of Ni and YIG wires used in the calculations.

		Wire material	
Property	Symbol (units)	Ni	YIG
Saturation magnetization	M_s (kA/m)	460	140
Spectroscopic splitting factor	g	2.2	2
Gilbert damping constant	α	0.03	0.005
Drude conductivity	σ_w (Ω^{-1} m^{-1})	1.5×10^7	
Relative intrinsic permittivity	ϵ_w/ϵ_0	$i\sigma_w/\omega\epsilon_0$	$15(1+0.001i)$

formulation based on the shape demagnetizing tensor $\overleftrightarrow{N}_d$ of Eq. (66). In such a case, the FMR behavior of wire arrays can be alternatively described by $\overleftrightarrow{N}_{\text{eff}}$ or $\overleftrightarrow{N}_d$.

C. Quasistatic regime and effective demagnetizing tensors

Ferromagnetic resonance studies of nanowire arrays usually fall in the limit $|k_w|a \ll 1$, corresponding to a QS response of the individual wires.[31–35] In this case, the components of $\overleftrightarrow{\eta}_{\text{eff}}$ reduce to η_{eff} and $\eta_{\text{eff},t}$. Explicit expressions for these can be obtained in the monopolar regime by substituting Eqs. (28a) and (28b) into Eq. (64), resulting in

$$\eta_{\text{eff}} = \frac{f\omega_M[\omega_H^* + (1-f)\omega_M/2]}{[\omega_H^* + (1-f)\omega_M/2]^2 - \omega^2}, \tag{70a}$$

$$\eta_{\text{eff},t} = \frac{f\omega_M\omega}{[\omega_H^* + (1-f)\omega_M/2]^2 - \omega^2}. \tag{70b}$$

In the low-damping limit, these components have a pole at

$$\omega_{r,\text{eff}} = \omega_H + \frac{\omega_M}{2}(1-f) = \omega_0 + \frac{\omega_M}{2}(1-3f), \tag{71}$$

corresponding to the uniform-mode FMR frequency of an ensemble of interacting wires in the QS limit. In Eq. (71), $\omega_H = \omega_0 - f\omega_M$ is the static field inside the wires in units of angular frequency, where $\omega_0 = \mu_0|\gamma|H_{\text{ext0}}$ accounts for the externally applied field and $-f\omega_M$ represents the axial interwire dipolar field. This result was initially proposed in Ref. 31, based on phenomenological arguments, and subsequently recovered from a formal expression for interwire interactions.[35]

In Ref. 35, the total demagnetizing tensor $\overleftrightarrow{N}$ of the array, including the interaction tensor $\overleftrightarrow{N}_{\text{int}}$, was expressed as

$$\overleftrightarrow{N} = \overleftrightarrow{N}_w + \overleftrightarrow{N}_{\text{int}}, \tag{72}$$

implying that locally, the field $\mathbf{h}_w$ inside the individual wires differs from the external field $\mathbf{h}_{\text{ext}}$ imposed on the array due to the intrawire and interwire dipolar interactions accounted for by the tensors $\overleftrightarrow{N}_w$ and $\overleftrightarrow{N}_{\text{int}}$, respectively. Then, substituting Eq. (32) into Eq. (64) yields

$$\left(\frac{\overleftrightarrow{\eta}_{\text{eff}}}{f}\right)^{-1} = \overleftrightarrow{\chi}_w^{-1} + \overleftrightarrow{N}, \tag{73}$$

thereby indicating that in the QS limit, it is the demagnetizing tensor $\overleftrightarrow{N}$ that connects the intrinsic susceptibility $\overleftrightarrow{\chi}_w$ of the individual wires to the effective external response $\overleftrightarrow{\eta}_{\text{eff}}$ of an array of interacting wires.

Alternatively, assuming that $\overleftrightarrow{N}_{\text{eff}} = \overleftrightarrow{N}_d$ holds and combining Eqs. (65) and (72), we obtain

$$\overleftrightarrow{N} = (1-f)\overleftrightarrow{N}_w + f\overleftrightarrow{N}_d, \tag{74}$$

where the tensor $\overleftrightarrow{N}$ is now interpreted as a simple linear interpolation between $\overleftrightarrow{N}_w$ and $\overleftrightarrow{N}_d$, corresponding to a dilute ensemble of noninteracting wires (when $f=0$) and to a homogeneously magnetized thin disk with the shape of the array (when $f=1$), respectively. In particular, at $f=1/3$ we have $\overleftrightarrow{N} = \overleftrightarrow{I}/3$ and Eq. (73) predicts an isotropic FMR response of the array.[31]

Equation (74) was initially established in Ref. 81 within a mean-field approach based on magnetostatic energy considerations, in order to study FMR in particulate magnetic recording tapes. This model has subsequently been applied or extended to study various magnetic heterostructures.[82–86] Again, when the length L of the wires is much larger than both their diameter d and separation D (i.e., when $\overleftrightarrow{N}_{\text{eff}} = \overleftrightarrow{N}_d$), the macroscopic formulation for $\overleftrightarrow{N}$ leading to Eq. (74) becomes rigorously equivalent to our interaction approach, resulting in Eq. (72).

V. APPLICATION OF THE MODEL AND DISCUSSION

Having established the general formalism for the effective magnetic response of composite materials based on ferromagnetic wires, we are now in a position to study how electromagnetic size effects associated with retardation modify the magnetic properties of single and arrays of wires, as well as to clarify the conditions for which the latter display a region of negative effective permeability. The results of our model are applied to Ni wires with representative intrinsic properties, as given in Table II (ϵ_0 is the permittivity of free space). Unless otherwise stated, these parameters are used in all the calculations presented below. Table II also provides the properties of insulating yttrium iron garnet (YIG) wires, which will be used in Sec. V B.

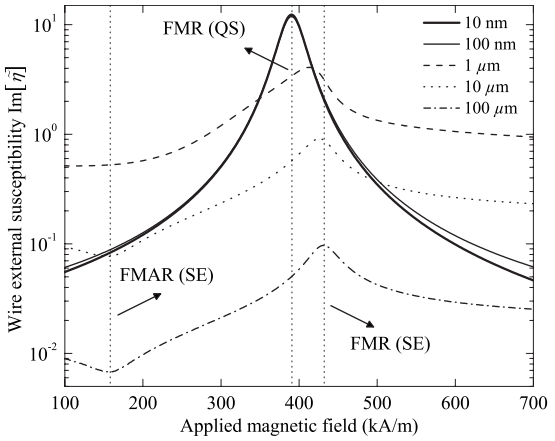

FIG. 3. Imaginary part of the diagonal component $\tilde{\eta}$ of the external susceptibility tensor of the wire as a function of the applied magnetic field, at 24 GHz, for a single Ni wire of varied radius ranging from 10 nm to 100 μm. The curves are calculated using Eq. (26) with the parameters given in Table II. The vertical dotted lines indicate the fields satisfying the FMR condition in the QS limit [Eq. (29)] and the FMR and FMAR conditions in the SE limit [Eqs. (38) and (39), respectively].

A. Influence of electromagnetic size effects on the FMR parameters of a single Ni wire

Electromagnetic size effects associated with the screening and damping of eddy currents can significantly modify the dispersion and dissipation characteristics of ferromagnetic-metallic wires. To illustrate this, we first consider a Ni wire of radius a located in free space, brought to saturation by an axial static magnetic field $\mathbf{H}_{\text{ext0}}$, and subjected to a transverse dynamic magnetic field $\mathbf{h}_{\text{loc}}$ with a frequency of $\omega/2\pi = 24$ GHz (corresponding to a nonmagnetic skin depth $\delta_{w0} = 0.84$ μm). The microwave magnetic field excites the wire in the mode $n = \pm 1$, leading to a magnetization response $\langle \mathbf{m}_w \rangle = \overleftrightarrow{\eta}_w \mathbf{h}_{\text{loc}}$ governed by Eqs. (25) and (26). Experimentally, this is realized by placing the wire in a resonant cavity with its axis perpendicular to the linearly polarized microwave magnetic field of an unperturbed cavity mode and by measuring the power absorbed by the sample as a function of the applied static field.[42,43,87] In this configuration and assuming that perturbation theory holds, the measured complex frequency shift of the cavity is proportional to the diagonal component $\tilde{\eta}$ of the external susceptibility tensor,[40] the imaginary part of which reflects the absorption of electromagnetic waves by the sample.

Figure 3 shows the imaginary part of $\tilde{\eta}$, calculated using Eq. (26), as a function of the applied static magnetic field (100–700 kA/m) for a single Ni wire of varied radius ranging from 10 nm to 100 μm. The theoretical spectra illustrate how skin effect modifies the FMR and FMAR conditions, as well as the width, shape, and amplitude of the absorption curve (note that the scale for Im$[\tilde{\eta}]$ is logarithmic). The general trends are further summarized in Fig. 4, which shows the dependence of the main FMR parameters on the normalized radius a/δ_{w0}, extending between the size-independent limits of weak ($a/\delta_{w0} \lesssim 0.1$) and strong ($a/\delta_{w0} \gtrsim 50$) skin effect.

In the QS limit, the incident magnetic field penetrates the entire wire and excites uniform oscillations of the magnetization. The external susceptibility reduces to η given by Eq. (28a) so that the FMR field satisfies Eq. (29) and no local minimum is observed at the FMAR field. The resonance linewidth does not vary with a/δ_{w0} and increases linearly with the value of the Gilbert damping parameter, as shown in Figs. 4(c) and 4(d), respectively. In the SE limit, the screening effect due to eddy currents confines the interior fields within the skin depth $\delta_w \ll a$. The external susceptibility $\tilde{\eta}$ reduces to Eq. (36) so that it is directly related to the surface impedance ζ_w of Eq. (37), which accounts for both the metallic and gyrotropic natures of the wire intrinsic properties. In particular, the FMR and FMAR conditions satisfy Eqs. (38) and (39), respectively, while the absorption and linewidth are governed by the real part of ζ_w.

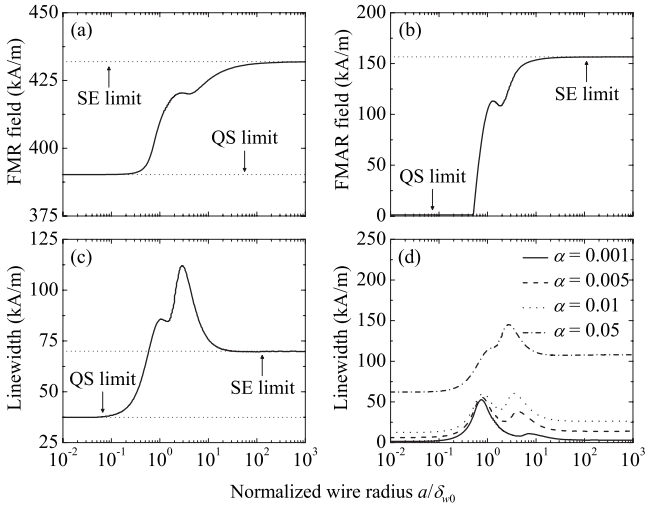

FIG. 4. Dependence of the FMR parameters on the normalized radius a/δ_{w0} for a Ni wire at 24 GHz ($\delta_{w0} = 0.84$ μm). (a) FMR field, (b) FMAR field, and (c) resonance linewidth. Results are calculated using Eq. (26) with the parameters given in Table II. The values expected in the size-independent QS and SE limits are indicated by the horizontal dotted lines. (d) The same as (c) but for four different values of the Gilbert damping parameter α.

Increasing a/δ_{w0} in the intermediate regime between the QS and SE limits progressively transforms the uniform resonance mode into a surface mode, thereby introducing a nontrivial $k_w a$ dependence to $\tilde{\eta}$, which strongly modifies the FMR parameters. First, the absorption curve loses its symmetrical Lorentzian line shape and exhibits a strong reduction in amplitude (Fig. 3). Then, as illustrated in Figs. 4(a) and 4(b), the FMR field increases from the uniform-mode value of an axially magnetized cylinder to that of parallel resonance in metals [Eqs. (29) and (38), respectively] while the FMAR manifests itself as a minimum in the absorption curve, beginning at $a/\delta_{w0} \approx 0.5$ and rapidly increasing to the field value satisfying Eq. (39). Likewise, Fig. 3 shows that the FMAR becomes clearly noticeable in the absorption curve for $a \geq 10$ μm. Further, the curves in Figs. 4(c) and 4(d) indicate that the linewidth reaches its maximum value when $1 \lesssim a/\delta_{w0} \lesssim 10$, owing to the significant damping produced by the eddy currents generated inside the skin depth. This contribution does not arise in the QS and SE limits. In the former, the damping is governed by the intrinsic mag-

netic losses and the screening effect of eddy currents is negligible while in the latter, the incident field hardly penetrates into the volume of the conductor so that bulk eddy currents are not involved in the absorption of electromagnetic energy.[88]

The behavior of the FMR parameters in the transition regime $1 \lesssim a/\delta_{w0} \lesssim 10$ can be interpreted on the basis that the EQS external susceptibility $\tilde{\eta}$ becomes a complex $k_w a$-dependent function arising from the strong coupling between a volume mode and a surface mode, which have different FMR parameters but comparable and interrelated contributions to the linewidth. As a result, the FMR parameters also display some irregularities in the transition region, as shown in Fig. 4 by the slight drop in the otherwise monotonic increase in the FMR and FMAR fields and by the double-peak structure in the linewidth, which was also predicted in Ref. 42. Finally, we must emphasize that the exact values chosen for the properties M_s, g, α, and σ_w do not significantly influence the general features of the external susceptibility spectra, shown in Fig. 3.

B. Renormalized permeability of magnetic wires: Comparison between conductors and insulators

Our general formalism, which has so far focused on *conducting* wires, applies equally well to gyromagnetic *insulators* (e.g., ferrites), characterized by a permittivity ϵ_w and a wave vector k_w that are mostly real at microwave frequencies. In this case, as will be examined below, the $k_w a$-dependent renormalized permeability exhibits a resonant behavior and may become negative in certain frequency ranges due to the excitation of magnetic dipole resonances inside the individual wires. Recently, several studies[67,72,78,89–94] have proposed that such localized dipole resonances in arrays of subwavelength high-permittivity inclusions may provide a route to achieve negative index metamaterials with negative effective constitutive parameters. In this section, we examine the influence of the permittivity ϵ_w on the $k_w a$-dependent gyromagnetic response, by comparing the renormalized permeability $\tilde{\mu}_\perp = \mu_\perp G(k_w a)$ [Eq. (23)] of two materials with similar gyromagnetic responses, but very distinct dielectric properties.

We consider a conducting Ni ($a=2$ μm) and an insulating YIG ($a=2$ mm) magnetic wires with intrinsic parameters given in Table II. For these parameters, the frequency at which $|k_w|a \approx 1$ is close to the FMR frequency of $\mu_\perp$ [Eq. (38)] for both materials. This results in a strong interaction between the gyromagnetic and $k_w a$-dependent responses and thus in a substantial modification of $\tilde{\mu}_\perp$ compared to $\mu_\perp$. Figure 5 compares the frequency dependence (1–40 GHz) of various permeability response functions of single Ni (left panel) and YIG (right panel) wires at constant static magnetic field $H_{\text{ext}0} = \frac{1}{2} M_s$ applied parallel to the wire axis. First, we show in Fig. 5(a) the spectra of the relative intrinsic permeability component $\mu_\perp/\mu_0$ [Eq. (15)]. The influence of the wire intrinsic permittivity alone on the renormalized permeability is then examined in Fig. 5(b), which shows $G(k_{w0}a)$ for nonmagnetic wires with dielectric properties identical to those of Ni and YIG. This is achieved by setting

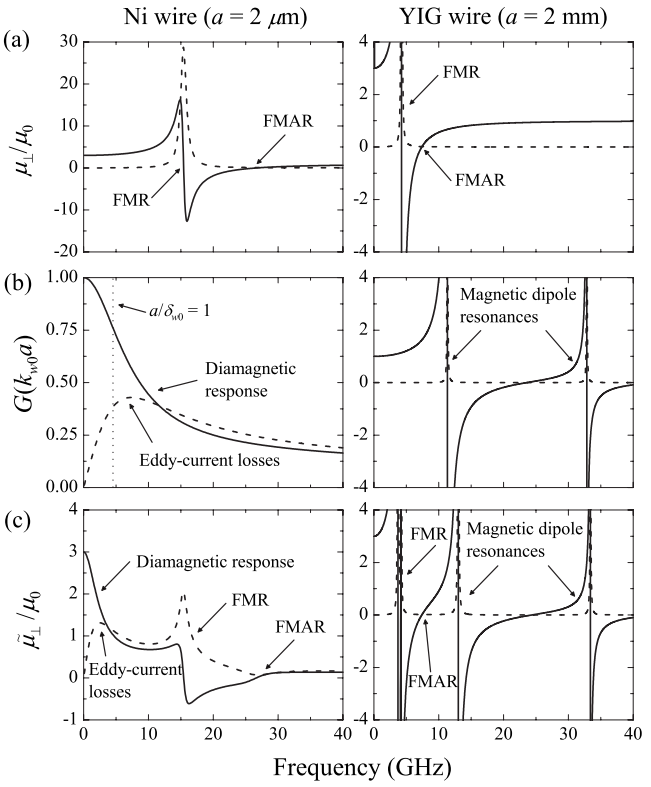

FIG. 5. Frequency dependence of various permeability response functions of single Ni ($a=2$ μm, left panel) and YIG ($a=2$ mm, right panel) wires with intrinsic parameters given in Table II. (a) Relative intrinsic permeability component $\mu_\perp/\mu_0$ at constant static magnetic field $H_{\text{ext}0} = \frac{1}{2} M_s$ applied along the wire axis. (b) Renormalization factor $G(k_{w0}a)$ for nonmagnetic wires with dielectric properties identical to those of Ni and YIG. (c) Relative renormalized permeability component $\tilde{\mu}_\perp/\mu_0$ at constant static magnetic field $H_{\text{ext}0} = \frac{1}{2} M_s$ applied along the wire axis. Real and imaginary parts are denoted by solid and dashed lines, respectively.

$\mu_\perp = \mu_0$ in Eqs. (13) and (23) so that $\tilde{\mu}_\perp = \mu_0 G(k_{w0}a)$, where $k_{w0} = \omega\sqrt{\epsilon_w \mu_0}$ is the nonmagnetic wave vector. Hence, $G(k_{w0}a) = \tilde{\mu}_\perp/\mu_0$ shown in Fig. 5(b) corresponds to the relative $k_{w0}a$-dependent renormalized permeability of a *nonmagnetic* wire. Finally, Fig. 5(c) shows $\tilde{\mu}_\perp/\mu_0$, which illustrates the combined gyromagnetic and $k_w a$-dependent responses of single Ni and YIG wires.

We find that both intrinsic magnetic responses exhibit a Lorentzian profile with position, width, and amplitude determined by the applied field $H_{\text{ext}0}$ and the magnetic properties (M_s, g, and α) of Ni and YIG [Fig. 5(a)]. As ω tends to 0, we note that $\mu_\perp/\mu_0 \approx 1 + M_s/H_{\text{ext}0} = 3$ for both Ni and YIG, which follows from Eq. (15) with $\omega=0$ and $\omega_H = \omega_0$. However, while the intrinsic permeability $\mu_\perp$ has the same dispersive behavior for the two materials, their respective $k_{w0}a$-dependent response $G(k_{w0}a)$ differs significantly, as shown in Fig. 5(b). In the left panel, the metallic wire, with wave vector $k_{w0} = (1+i)/\delta_{w0}$, exhibits a relaxationlike behavior. The screening effect of eddy currents leads to a monotonic decrease in the real part of $G(k_{w0}a)$ in the transition regime $\delta_{w0} \approx a$, which is reduced from 1 at low frequencies (dielectriclike behavior) to 0 at high frequencies (superconductinglike behavior). Likewise, eddy-current damping is ac-

counted for by the imaginary part of $G(k_{w0}a)$, which vanishes for $\omega=0$, increases as $(a/\delta_{w0})^2 \propto \omega$ at low frequencies, reaches a maximum when $\delta_{w0} \approx a$, and decreases as $(a/\delta_{w0})^{-1} \propto \omega^{-1/2}$ at high frequencies. In the right panel, the response $G(k_{w0}a)$ of the insulating wire displays a multiresonant character, owing to the excitation of magnetic dipole resonances (Mie-type resonances) inside the cylindrical wire. The resonance frequencies correspond to the poles of $G(k_{w0}a)$, which occur whenever the condition $k_{w0}aJ_0(k_{w0}a) = J_1(k_{w0}a)$ is fulfilled for $|k_{w0}|a \gtrsim 1$. These dimensional resonances are accompanied by a maximum of $\mathrm{Im}[G(k_{w0}a)]$ and a change in sign of $\mathrm{Re}[G(k_{w0}a)]$. The latter thus becomes negative in a small frequency range on the high-frequency side of each pole. The strength and width of the resonances are controlled by dielectric losses so that increasing $\mathrm{Im}[\epsilon_w]$ damps out the resonant behavior of $G(k_{w0}a)$ and ultimately restricts $\mathrm{Re}[G(k_{w0}a)]$ to positive values. Further, when the condition $|\mathrm{Im}[\epsilon_w]| \gg |\mathrm{Re}[\epsilon_w]|$ is reached, the spectrum of $G(k_{w0}a)$ transforms to that of a conducting wire, which shows no resonant character at $\delta_{w0} \approx a$.

As expected, these ϵ_w-dependent features are also present in the renormalized gyromagnetic response, as shown in Fig. 5(c). In the left panel, the intrinsic gyromagnetic response of Ni remains apparent in the renormalized permeability but eddy currents bring significant modifications to the spectrum of $\tilde{\mu}_\perp/\mu_0$ compared to that of $\mu_\perp/\mu_0$. The diamagnetic screening reduces the real part of $\tilde{\mu}_\perp/\mu_0$ considerably with increasing frequency so that the permeability level remains smaller than 1 (even near the FMR) and decreases toward 0 at high frequency. Likewise, eddy-current losses lead to a new peak in the imaginary part of $\tilde{\mu}_\perp/\mu_0$ and to an overall broadening and decrease in amplitude of the FMR peak. In the right panel, the renormalized permeability of the YIG wire consists essentially in the intrinsic gyromagnetic response, on which is superimposed the series of magnetic dipole resonances of the single wire at frequencies satisfying the condition $k_waJ_0(k_wa)=J_1(k_wa)$. The response thus exhibits several regions of negative renormalized permeability, the spectral positions of which can be controlled, to a certain extent, by varying the static magnetic field.

In the context of studies of metamaterials with a negative refractive index, ensembles of insulating ferrimagnetic wires have been predicted to display a magnetic-field-tunable range of negative effective permeability at microwave frequencies.[9,10] However, it must be emphasized that in order to support magnetic dipole resonances in the frequency range where the intrinsic permeability also exhibits a resonant character, the condition $|k_w|a \approx 1$ must be fulfilled at microwave frequencies. This generally requires ferrimagnetic wires with a fairly large radius (i.e., $a \gtrsim 1$ mm) so that the homogeneity assumption $|k_m|a \ll 1$ may not be strictly respected in such composite materials. In contrast, using arrays of submicron wires of ferromagnetic metals ensures that $|k_m|a \ll 1$ is rigorously satisfied while permitting higher operating frequencies and still minimizing eddy-current losses.

C. Arrays of wires and negative effective permeability

In addition to the limitations imposed by electromagnetic retardation inside the individual wires, the effective magnetic response $\overleftrightarrow{\tilde{\mu}}_{\mathrm{eff}}$ of an ensemble of interacting wires is also reduced due to the effect of diluting the wires in the host medium. This may eventually prevent the real part of the effective permeability from becoming negative, which is essential for the development of left-handed metamaterials. We now address this issue. Consider an array of axially magnetized Ni wires with properties given in Table II, filling the pores of a dielectric thin-film matrix of permittivity $\epsilon_m=10\epsilon_0$, permeability $\mu_m=\mu_0$, and infinite lateral extent. The wires occupy a volume fraction $f=0.20$ of the array and are brought to saturation by an axial static magnetic field $H_{\mathrm{ext}0}=\frac{1}{2}M_s$. The total static field H_{w0} inside the individual wires includes an additional contribution from the static dipolar interaction field so that $H_{w0}=H_{\mathrm{ext}0}-fM_s$ (monopolar regime) and thus $\omega_H=\omega_0-f\omega_M$, as in Sec. IV C.

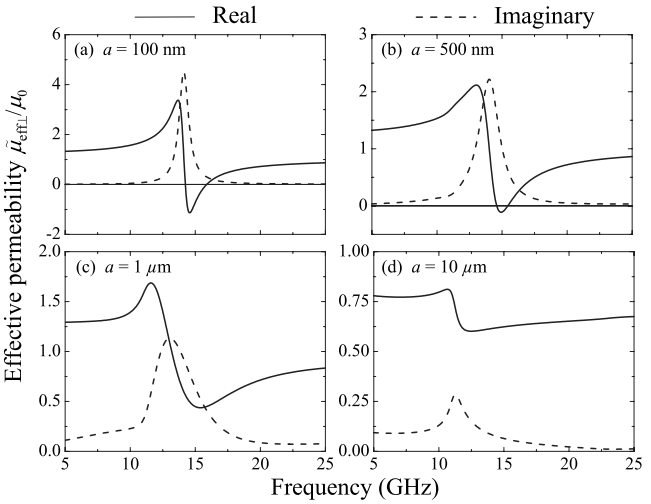

FIG. 6. Real and imaginary parts of the relative effective permeability component $\tilde{\mu}_{\mathrm{eff}\perp}/\mu_0$ as a function of frequency for an array of Ni wires of radius (a) 100 nm, (b) 500 nm, (c) 1 μm, and (d) 10 μm. The spectra correspond to theoretical calculations using Eq. (54) with $H_{\mathrm{ext}0}=\frac{1}{2}M_s$, $f=0.20$, and the Ni wire parameters given in Table II. Real and imaginary parts are denoted by solid and dashed lines, respectively.

We consider a wave propagating in the plane of the array with its electric and magnetic fields oriented along and transverse to the wire axis, respectively. In the case of an infinite array, this mode is characterized by the effective scalar permeability $\tilde{\mu}_{\mathrm{eff}\perp}$ of Eq. (54) with $\tilde{\eta}$ and $\tilde{\eta}_t$ calculated using Eq. (26). We emphasize that using $\tilde{\mu}_{\mathrm{eff}\perp}$ is rigorously valid only in the case of *unbounded* arrays. For *guided* waves propagating in a finite-size structure (e.g., a transmission line), $\tilde{\mu}_{\mathrm{eff}\perp}$ cannot be used directly as the characteristic permeability that enters the propagation constant of the structure so that the full expression for $\overleftrightarrow{\tilde{\mu}}_{\mathrm{eff}}$ may be required.[76,95] Further, even for infinite arrays, $\tilde{\mu}_{\mathrm{eff}\perp}$ applies to this mode of propagation only so that other configurations may involve the explicit expressions of the diagonal and off-diagonal components of $\overleftrightarrow{\tilde{\mu}}_{\mathrm{eff}}$.

The frequency dependence of the real and imaginary parts of $\tilde{\mu}_{\mathrm{eff}\perp}/\mu_0$ is illustrated in Fig. 6 for an array of Ni wires of various radii. In Fig. 6(a), $a=100$ nm and the QS approximation holds so that $\tilde{\eta}$ and $\tilde{\eta}_t$ are given by Eq. (28). In this

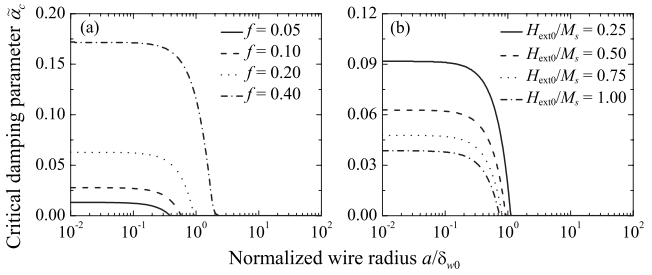

FIG. 7. Critical damping parameter $\tilde{\alpha}_c$ of a Ni wire array as a function of the normalized wire radius a/δ_{w0}. (a) $H_{ext0}/M_s=0.50$ and f ranges between 0.05 and 0.40. (b) $f=0.20$ and H_{ext0}/M_s ranges between 0.25 and 1.00. The Ni wire parameters are given in Table II and δ_{w0} refers here to the nonmagnetic skin depth of Ni at 24 GHz. The critical damping $\tilde{\alpha}_c$ corresponds to the maximum value for α allowing the real part of $\tilde{\mu}_{\text{eff}\perp}$ to become negative between the FMR and FMAR frequencies.

case, $\tilde{\mu}_{\text{eff}\perp}$ has a Lorentzian profile characterized by the FMR and FMAR frequencies, between which the real part becomes negative. As the size of the wires is increased, the response of the individual wires falls in the EQS regime so that the FMR gradually shifts to lower frequency and the absorption curve progressively broadens, decreases in amplitude, and becomes asymmetrical. In this regime, the frequency behavior of the FMR parameters of $\tilde{\mu}_{\text{eff}\perp}$ becomes a complicated function of the intrinsic properties of the wires, the geometrical parameters of the array, and the applied static magnetic field. In the case of strong skin effect ($\sigma_w \to \infty$), the wires behave as perfect diamagnets with $\tilde{\eta} \approx -2$ and $\tilde{\eta}_t \approx 0$ so that Eq. (54) reduces to the material-independent value $\tilde{\mu}_{\text{eff}\perp}/\mu_0=(1-f)/(1+f)\approx 0.67$, which decreases with f and accounts for the fact that the average magnetic induction is completely excluded from the interior of the wires.

We observe that when the radius of the wires exceeds a certain value (between $a=500$ nm and 1 μm in the present case), the effective damping acting on the wires becomes sufficiently strong to restrict the real part of $\tilde{\mu}_{\text{eff}\perp}$ to positive values in the whole frequency range. Hence, the transition to the EQS regime at $a/\delta_{w0} \approx 1$ not only invalidates the assumption of uniform-mode oscillations inside the individual wires but also prevents the effective permeability from becoming negative, regardless of the intrinsic magnetic losses α. Therefore, several studies[25–28] investigating negative refraction in arrays of ferromagnetic-metallic wires with $a > 1$ μm were developed within the unjustified QS approximation.

In cases where the value of a/δ_{w0} does not *a priori* forbid negative permeability, there exists a critical value $\tilde{\alpha}_c$ for the Gilbert damping parameter, above which the real part of $\tilde{\mu}_{\text{eff}\perp}$ remains positive at all frequencies. This is illustrated in Fig. 7, which shows the dependence of $\tilde{\alpha}_c$ on a/δ_{w0} for an array of Ni wires with parameters of Table II and $\delta_{w0}=0.84$ μm (nonmagnetic skin depth of Ni at 24 GHz). The critical damping was extracted from spectra of $\tilde{\mu}_{\text{eff}\perp}$ calculated using Eq. (54). In Fig. 7(a), $H_{ext0}/M_s=0.50$ and the volume fraction f ranges between 0.05 and 0.40 while in Fig. 7(b), $f=0.20$ and H_{ext0}/M_s extends from 0.25 to 1.00. The curves indicate that the value of $\tilde{\alpha}_c$ increases with increasing f and decreasing H_{ext0}/M_s so that negative effective permeability is favored in dense nanowire arrays that can be saturated at fairly low applied fields. As discussed above, when $a/\delta_{w0} \gtrsim 1$, the effective permeability never becomes negative, even in the idealized case of a dense array of lossless wires (i.e., $f=0.40$ and $\alpha=0$).

It does not seem possible to determine a general analytical expression for the critical damping $\tilde{\alpha}_c$ of $\tilde{\mu}_{\text{eff}\perp}$ in the EQS regime. However, in the QS limit, $\tilde{\alpha}_c$ reduces to the size-independent value α_c and it can be shown (see Appendix B) that

$$\alpha_c = \alpha_{c0} - \sqrt{\alpha_{c0}^2 - 1}, \tag{75}$$

where

$$\alpha_{c0} = \frac{2}{f}\left[\frac{H_{ext0}}{M_s} + \frac{(1-2f)}{2}\right]. \tag{76}$$

The QS critical damping depends on f and H_{ext0}/M_s only and corresponds to the size-independent portion of the curves shown in Fig. 7. Equation (75) thus yields an intrinsic threshold value for α_c, below which negative effective permeability is theoretically possible in infinite arrays of ferromagnetic wires. For example, a fairly dense nanowire array (e.g., $f=0.30$) subjected to a relatively small applied field (e.g., $H_{ext0}/M_s=0.25$) yields the critical value $\alpha_c \approx 0.17$, which is larger than the typical values of α expected for ferromagnetic metals (i.e., with α in the range 0.001–0.05, see Ref. 40). This indicates that arrays of axially magnetized metallic nanowires with realistic parameters may exhibit a negative magnetic response between the FMR and FMAR frequencies of the effective permeability.

VI. FURTHER DISCUSSION AND SUMMARY

This work establishes a model for the effective permeability tensor of arrays of axially magnetized ferromagnetic wires. The model begins by considering the intrinsic properties of a single wire and proceeds to the effective external response of a finite-size array of interacting wires. It employs a multiscale approach, which effectively connects four hierarchical levels, summarized in Table I. This hierarchical structure establishes the influence of the various parameters and hypotheses involved at each step of the derivation, thereby allowing one to introduce modifications at all levels. For instance, owing to the symmetry of Maxwell's equations, the method can readily be adapted to yield the $k_w a$-dependent effective permittivity tensor $\vec{\epsilon}_{\text{eff}}$ of arrays of axially magnetized wires having an intrinsic *gyroelectric* permittivity tensor $\vec{\epsilon}_w$ and being subjected to a dynamic electric field polarized perpendicular to their axis. Such a result could be applied to the study of the magneto-optical response of ferromagnetic nanowire arrays.[23,24]

Another direct extension of the model would be the inclusion of different types of magnetocrystalline anisotropy as an effective demagnetizing tensor $\vec{N}_{\text{mca}}$ in the equation of motion for the magnetization[40] in order to yield more general expressions for the components of the intrinsic permeability tensor $\vec{\mu}_w$. Further, in the QS limit, magnetocrystalline aniso-

tropy can be accounted for simply by replacing the shape demagnetizing tensor $\vec{\vec{N}}_w$ by $\vec{\vec{N}}_w+\vec{\vec{N}}_{\mathrm{mca}}$, whenever it appears in the QS equations [e.g., Eqs. (32), (56), and (73)]. Likewise, the gyromagnetic external susceptibility tensor $\vec{\vec{\eta}}_w$ of a single wire embedded in a host medium, which is the main parameter entering the Maxwell-Garnett mixing rule, could alternatively be used in the Bruggeman formalism.[44] However, in this latter case, the self-consistent homogenization condition would not yield compact and explicit expressions for the components of the effective permeability tensor.

An important simplifying assumption made throughout the present work is that the exchange interaction and, consequently, exchange-conductivity effects are neglected. These effects may arise in ferromagnetic metals due to the excitation of spin waves by the strongly nonuniform dynamic magnetic field inside the skin depth, which leads to a nonlocal (i.e., wave-vector-dependent) intrinsic permeability, as well as to a broadening and shift of the FMR absorption curve.[96] A general theory of FMR in thin metallic wires based on the simultaneous solution of Maxwell's equations and the equation of motion for the magnetization including the exchange interaction was proposed by Kraus.[43] He derived fairly complex expressions for the surface impedance and relative absorption of the individual resonance modes (including the mode $n=\pm 1$) and studied the size dependence of the FMR parameters. His approach thus fully incorporates the effect of the exchange interaction on the response of a single ferromagnetic wire. However, due to the nonlocal response and the resulting additional boundary conditions on the magnetization, his model does not readily lend itself to the derivation of an external susceptibility tensor $\vec{\vec{\eta}}_w$ in terms of renormalized permeability components $\tilde{\mu}$ and $\tilde{\mu}_t$, which would account for the exchange interaction. Then, Eq. (50) could not be used directly for the determination of $\vec{\vec{\mu}}_{\mathrm{eff}}$ in terms of $\vec{\vec{\eta}}_w$ and the treatment of arrays of wires.

Our neglect of the exchange interaction in the equation of motion for the magnetization may be justified as follows. In the QS limit, the skin depth remains much larger than the wire radius and uniform oscillations of the magnetization are excited so that exchange-conductivity effects are obviously absent. Less intuitive is their neglect in the regime of strong skin effect. It was shown, in relation to the modeling of giant magnetoimpedance in microwires and ribbons, that such exchange-conductivity effects become significant only at subgigahertz frequencies.[71,97] As the present work focuses primarily on the $k_w a$ dependence of $\vec{\vec{\eta}}_w$ induced by the electromagnetic skin effect in the range 1–100 GHz, we decided to avoid the analytical complexity introduced by the exchange interaction in the electromagnetic behavior of ferromagnetic metals. Therefore, excitation of exchange-spin and magnetostatic modes in the individual wires is implicitly excluded from the present study. Further, generalizing our expression for $\vec{\vec{\eta}}_w$ in order to include the magnetostatic modes of an axially magnetized cylinder[98] or exchange-conductivity effects is possible *a priori* but not straightforward. In this respect, a starting point to incorporate the exchange-conductivity mechanism as a correction factor to our renormalization procedure may be found in Ref. 71 [see Eqs. (91) and (92) therein]. Likewise, spin-wave excitations in arrays of ferromagnetic nanowires studied by Brillouin light scattering[37,39] could alternatively be explained by extending our formalism for $\vec{\vec{\mu}}_{\mathrm{eff}}$.

Another simplification of the model is the requirement that the static field and magnetization lie parallel to the axis of the wires and perpendicular to the radial wave vector k_w. This symmetrical configuration allows one to use the method of separation of variables in cylindrical coordinates in the scattering problem that must be solved to yield $\vec{\vec{\eta}}_w$. Generalization of our formalism based on deriving renormalized permeability components $\tilde{\mu}$ and $\tilde{\mu}_t$ to other inclusion shapes, such as arrays of spherical inclusions,[51–54,57–60] poses significant challenges. Indeed, the scattering of a plane electromagnetic wave by a gyrotropic sphere has not been solved in closed analytical form because Maxwell's equations are then no longer separable.[99] Likewise, extending our EQS approach to static fields at arbitrary angles to the wire axis suffers from similar difficulties. However, we must emphasize that in the QS limit, Eq. (32) for $\vec{\vec{\eta}}_w$ remains valid irrespective of the static field orientation, provided the appropriate rotation matrix is used to express $\vec{\vec{\chi}}_w$ and $\vec{\vec{N}}_w$ in the same coordinate system.

In summary, we have proposed a theory for the effective magnetic response of saturated arrays of axially magnetized ferromagnetic-metallic wires. We have established compact renormalized expressions for the components of the wire external susceptibility tensor $\vec{\vec{\eta}}_w$, which include both the gyromagnetic and $k_w a$-dependent natures of the individual wire response and account for the influence of eddy currents and skin effect on the FMR parameters. The model then incorporates $\vec{\vec{\eta}}_w$ into a Maxwell-Garnett homogenization procedure to yield the diagonal and off-diagonal components of the effective permeability tensor $\vec{\vec{\mu}}_{\mathrm{eff}}$. Our work thus generalizes to gyromagnetic cylindrical inclusions the isotropic EQS formalism of Lewin, which constitutes one of the earliest attempts to incorporate electromagnetic retardation into the Maxwell-Garnett mixing rule. Further, the formalism extends and bridges existing theories of the electromagnetic response of ferromagnetic composite materials, which have derived for $\vec{\vec{\mu}}_{\mathrm{eff}}$ either tensorial relations restricted to the QS regime or scalar expressions including retardation within the magnetic inclusions but neglecting the gyrotropic nature of their permeability. Introducing the effective external susceptibility tensor $\vec{\vec{\eta}}_{\mathrm{eff}}$, along with the effective demagnetizing tensor $\vec{\vec{N}}_{\mathrm{eff}}$, allows one to treat the FMR response of finite-size arrays in which static and dynamic dipolar interactions cannot be neglected.

The present work applies equally well to magnetic insulators and thus yields valuable insights into the modeling of negative permeability metamaterials based on the excitation of dimensional magnetic dipole resonances in ensembles of insulating ferrimagnetic rods. Moreover, we have provided physical guidelines for designing metamaterials with a negative effective permeability based on arrays of ferromagnetic-metallic wires and have established intrinsic limitations related to the size of the wire and to Gilbert damping, which prevent the effective permeability from becoming negative. Finally, the present theory is relevant to the understanding and modeling of composite materials based on gyromagnetic

inclusions in the presence of retardation effects and is sufficiently general to be applied or extended to various systems of interest.

ACKNOWLEDGMENTS

The authors are indebted to Arthur Yelon for his careful reading of the manuscript, valuable discussions, and much appreciated suggestions for improvements. Christophe Caloz, Louis-Philippe Carignan, Christian Lacroix, and Gabriel Monette are also acknowledged for helpful comments on the manuscript. This work was supported by grants under NSERC (Canada) and FQRNT (Québec).

APPENDIX A: SCATTERING OF AN ELECTROMAGNETIC PLANE WAVE BY AN INFINITE GYROMAGNETIC CYLINDER

Based on the scattering geometry, it is convenient to express the incident fields in Eqs. (11) and (12) in terms of the elementary functions of the cylindrical coordinate system (ρ,ϕ,z). Using the Jacobi-Anger identity[100]

$$e^{iu\cos\phi}=\sum_{n=-\infty}^{\infty} i^n J_n(u)e^{in\phi} \tag{A1}$$

with $u\cos\phi=k_m\rho\cos\phi=k_m x$, we obtain

$$\mathbf{e}_{\mathrm{loc}}=e_{\mathrm{loc}}\sum_{n=-\infty}^{\infty} i^n J_n(k_m\rho)e^{in\phi}\hat{\mathbf{z}}, \tag{A2}$$

$$\mathbf{h}_{\mathrm{loc}}=h_{\mathrm{loc}}\sum_{n=-\infty}^{\infty} i^n\left[n\frac{J_n(k_m\rho)}{k_m\rho}\hat{\boldsymbol{\rho}}+iJ_n'(k_m\rho)\hat{\boldsymbol{\phi}}\right]e^{in\phi}, \tag{A3}$$

where the time dependence is absorbed into $e_{\mathrm{loc}}=e_{\mathrm{loc}0}e^{-i\omega t}$ and $h_{\mathrm{loc}}=h_{\mathrm{loc}0}e^{-i\omega t}$, $J_n(u)$ are Bessel functions of the first kind, and the prime denotes derivative with respect to the argument. The scattered fields must correspond to a wave that travels outward and vanishes at infinity. They are expressed in terms of Hankel functions of the first kind $H_n^{(1)}(u)$

$$\mathbf{e}_{\mathrm{scat}}=e_{\mathrm{loc}}\sum_{n=-\infty}^{\infty} i^n a_n H_n^{(1)}(k_m\rho)e^{in\phi}\hat{\mathbf{z}}, \tag{A4}$$

$$\mathbf{h}_{\mathrm{scat}}=h_{\mathrm{loc}}\sum_{n=-\infty}^{\infty} i^n a_n\left[n\frac{H_n^{(1)}(k_m\rho)}{k_m\rho}\hat{\boldsymbol{\rho}}+iH_n^{(1)\prime}(k_m\rho)\hat{\boldsymbol{\phi}}\right]e^{in\phi}, \tag{A5}$$

where a_n are the amplitude coefficients of the scattered wave. For the assumed incident electric field and scalar permittivity of the wire, the electric field $\mathbf{e}_w=e_w(\rho,\phi)\hat{\mathbf{z}}$ transmitted inside the wire remains strictly axial and satisfies the wave equation

$$\boldsymbol{\nabla}\times[\overleftrightarrow{\mu}_w^{-1}(\boldsymbol{\nabla}\times\mathbf{e}_w)]-\omega^2\epsilon_w\mathbf{e}_w=\mathbf{0}, \tag{A6}$$

where $\overleftrightarrow{\mu}_w^{-1}$ is the inverse of the permeability tensor of Eq. (3). Equation (A6) can then be written as a two-dimensional Poisson's equation in polar coordinates,

$$\frac{\partial^2 e_w}{\partial\rho^2}+\frac{1}{\rho}\frac{\partial e_w}{\partial\rho}+\frac{1}{\rho^2}\frac{\partial^2 e_w}{\partial\phi^2}+k_w e_w=0, \tag{A7}$$

where k_w is given by Eq. (13). The method of separation of variables allows us to express $\mathbf{e}_w$ as an infinite sum of cylindrical modes

$$\mathbf{e}_w=e_w(\rho,\phi)\hat{\mathbf{z}}=e_{\mathrm{loc}}\sum_{n=-\infty}^{\infty} i^n b_n J_n(k_w\rho)e^{in\phi}\hat{\mathbf{z}}, \tag{A8}$$

where b_n are the amplitude coefficients of the transmitted wave. The transmitted magnetic field is then obtained using the Maxwell-Faraday equation

$$\mathbf{h}_w=-\frac{i}{\omega}\overleftrightarrow{\mu}_w^{-1}(\boldsymbol{\nabla}\times\mathbf{e}_w)$$

$$=h_{\mathrm{loc}}\frac{\zeta_m}{\zeta_w}\sum_{n=-\infty}^{\infty} i^n b_n[C_n^{\rho}(k_w\rho)\hat{\boldsymbol{\rho}}+iC_n^{\phi}(k_w\rho)\hat{\boldsymbol{\phi}}]e^{in\phi}, \tag{A9}$$

where the wave impedance ζ_w is given by Eq. (14) and the coefficients $C_n^{\rho}(k_w\rho)$ and $C_n^{\phi}(k_w\rho)$ are defined as

$$C_n^{\rho}(k_w\rho)=n\frac{J_n(k_w\rho)}{k_w\rho}-\beta J_n'(k_w\rho), \tag{A10}$$

$$C_n^{\phi}(k_w\rho)=J_n'(k_w\rho)-n\beta\frac{J_n(k_w\rho)}{k_w\rho}, \tag{A11}$$

where $\beta=\mu_t/\mu$. Determining the unknown amplitude coefficients a_n and b_n requires one to satisfy the electromagnetic boundary conditions at the surface of the wire $(\rho=a)$ for the continuity of e_z and h_ϕ. Using the orthogonality of the cylindrical modes n, we get

$$J_n(k_m a)+a_n H_n^{(1)}(k_m a)=b_n J_n(k_w a), \tag{A12a}$$

$$J_n'(k_m a)+a_n H_n^{(1)\prime}(k_m a)=\frac{\zeta_m}{\zeta_w}b_n C_n^{\phi}(k_w a). \tag{A12b}$$

Solving Eqs. (A12a) and (A12b) for a_n and b_n yields

$$a_n=\frac{\zeta_m C_n^{\phi}(k_w a)J_n(k_m a)-\zeta_w J_n(k_w a)J_n'(k_m a)}{\zeta_w J_n(k_w a)H_n^{(1)\prime}(k_m a)-\zeta_m C_n^{\phi}(k_w a)H_n^{(1)}(k_m a)}, \tag{A13}$$

$$b_n=\frac{2i\zeta_w/\pi k_m a}{\zeta_w J_n(k_w a)H_n^{(1)\prime}(k_m a)-\zeta_m C_n^{\phi}(k_w a)H_n^{(1)}(k_m a)}, \tag{A14}$$

where the Bessel function Wronskian

$$J_n(k_m a)H_n^{(1)\prime}(k_m a)-J_n'(k_m a)H_n^{(1)}(k_m a)=\frac{2i}{\pi k_m a} \tag{A15}$$

was used to simplify the numerator of b_n. Note that when $\beta=0$, the coefficients a_n and b_n reduce, as expected, to the expressions valid for the scattering of a plane wave by an isotropic cylinder.[101]

TABLE III. Small-argument expansions of Bessel and Hankel functions and their derivatives of orders 0 and ±1.

Function	Expansion	Derivative	Expansion
$J_0(u)$	1	$J_0'(u)$	$-\frac{u}{2}$
$J_{\pm 1}(u)$	$\pm\frac{u}{2}$	$J_{\pm 1}'(u)$	$\pm\frac{1}{2}$
$H_0^{(1)}(u)$	$1+\frac{2i}{\pi}[\ln(\frac{u}{2})+\gamma_E]$	$H_0^{(1)\prime}(u)$	$-\frac{u}{2}+\frac{2i}{\pi u}$
$H_{\pm 1}^{(1)}(u)$	$\pm(\frac{u}{2}-\frac{2i}{\pi u})$	$H_{\pm 1}^{(1)\prime}(u)$	$\pm(\frac{1}{2}+\frac{2i}{\pi u^2})$

Under the conditions $|k_m|\rho \ll 1$ and $|k_m|a \ll 1$, we may replace all Bessel and Hankel functions and their derivatives with argument $k_m\rho$ or $k_m a$ in Eqs. (A2)–(A14) by their series expansions given in Table III in which $\gamma_E \approx 0.5772$ denotes Euler's constant.

APPENDIX B: CRITICAL DAMPING

We consider the effective permeability component $\tilde{\mu}_{\text{eff}\perp}$ in the QS limit, that is, $\tilde{\mu}_{\text{eff}\perp}=\mu_{\text{eff}\perp}$. We wish to determine the critical value α_c for the Gilbert damping parameter, below which the effective permeability $\mu_{\text{eff}\perp}$ exhibits a negative real part between the FMR and FMAR frequencies. In the QS approximation, the EQS components of $\vec{\vec{\eta}}_w$ reduce to η and η_t given by Eqs. (28a) and (28b), respectively, where $\omega_H^*=\omega_H-i\alpha\omega$ and $\omega_H=\omega_0-f\omega_M$. Substituting η and η_t into Eq. (54) yields

$$\frac{\mu_{\text{eff}\perp}}{\mu_0}=\frac{(\omega_{r,\text{eff}}^*+f\omega_M)^2-\omega^2}{\omega_{r,\text{eff}}^*(\omega_{r,\text{eff}}^*+f\omega_M)-\omega^2}, \tag{B1}$$

where $\omega_{r,\text{eff}}^*=\omega_{r,\text{eff}}-i\alpha\omega$ and $\omega_{r,\text{eff}}$ is given by Eq. (71). When the Gilbert damping parameter is sufficiently small, the condition $\text{Re}[\mu_{\text{eff}\perp}]=0$ is fulfilled at two frequencies given by

$$\omega_\pm=\frac{\sqrt{(\omega_{r,\text{eff}}+f\omega_M)[(1-\alpha^2)(2\omega_{r,\text{eff}}+f\omega_M)\pm\Delta\omega]}}{\sqrt{2}(1+\alpha^2)}, \tag{B2}$$

where

$$\Delta\omega=\sqrt{[(1-\alpha^2)f\omega_M]^2-16\alpha^2\omega_{r,\text{eff}}(\omega_{r,\text{eff}}+f\omega_M)} \tag{B3}$$

accounts for the separation between the FMR (ω_-) and FMAR (ω_+) frequencies. The frequencies merge at $\Delta\omega=0$, corresponding to a critical Gilbert damping parameter

$$\alpha_c=\alpha_{c0}-\sqrt{\alpha_{c0}^2-1}, \tag{B4}$$

where

$$\alpha_{c0}=\frac{2}{f}\left[\frac{H_{\text{ext}0}}{M_s}+\frac{(1-2f)}{2}\right] \tag{B5}$$

is controlled by the applied field $H_{\text{ext}0}$, the saturation magnetization M_s, and the volume fraction f. When $\alpha<\alpha_c$, the real part of the effective permeability $\mu_{\text{eff}\perp}$ exhibits a region where it becomes negative between the FMR and FMAR frequencies. However, when $\alpha>\alpha_c$, the real part of $\mu_{\text{eff}\perp}$ is always positive so that negative effective permeability is not observed.

*vincent.boucher@polymtl.ca
†david.menard@polymtl.ca

[1] C. Caloz and T. Itoh, *Electromagnetic Metamaterials: Transmission Line Theory and Microwave Applications* (Wiley, New York, 2005).
[2] *Metamaterials: Physics and Engineering Explorations*, edited by N. Engheta and R. W. Ziolkowski (Wiley, New York, 2006).
[3] A. K. Sarychev and V. M. Shalaev, *Electrodynamics of Metamaterials* (World Scientific, Singapore, 2007).
[4] *Metamaterials Handbook*, edited by F. Capolino (CRC Press, Boca Raton, 2009).
[5] S. T. Chui and L. Hu, Phys. Rev. B **65**, 144407 (2002).
[6] O. Reynet, A.-L. Adenot, S. Deprot, O. Acher, and M. Latrach, Phys. Rev. B **66**, 094412 (2002).
[7] D. P. Makhnovskiy and L. V. Panina, J. Appl. Phys. **93**, 4120 (2003).
[8] V. Boucher and D. Ménard, J. Appl. Phys. **103**, 07E720 (2008).
[9] S. Liu, W. Chen, J. Du, Z. Lin, S. T. Chui, and C. T. Chan, Phys. Rev. Lett. **101**, 157407 (2008).
[10] J. Jin, S. Liu, Z. Lin, and S. T. Chui, Phys. Rev. B **80**, 115101 (2009).
[11] W. Rotman, IRE Trans. Antennas Propag. **10**, 82 (1962).
[12] J. B. Pendry, A. J. Holden, W. J. Stewart, and I. Youngs, Phys. Rev. Lett. **76**, 4773 (1996).
[13] S. A. Schelkunoff and H. T. Friis, *Antennas: Theory and Practice* (Wiley, New York, 1952).
[14] J. B. Pendry, A. J. Holden, D. J. Robbins, and W. J. Stewart, IEEE Trans. Microwave Theory Tech. **47**, 2075 (1999).
[15] A. Encinas, M. Demand, L. Vila, L. Piraux, and I. Huynen, Appl. Phys. Lett. **81**, 2032 (2002).
[16] A. Saib, D. Vanhoenacker-Janvier, I. Huynen, A. Encinas, L. Piraux, E. Ferain, and R. Legras, Appl. Phys. Lett. **83**, 2378 (2003).
[17] A. Saib, M. Darques, L. Piraux, D. Vanhoenacker-Janvier, and I. Huynen, IEEE Trans. Microwave Theory Tech. **53**, 2043 (2005).
[18] B. Ye, F. Li, D. Cimpoesu, J. B. Wiley, J.-S. Jung, A. Stancu, and L. Spinu, J. Magn. Magn. Mater. **316**, e56 (2007).
[19] B. K. Kuanr, V. Veerakumar, R. L. Marson, S. R. Mishra, R. E. Camley, and Z. Celinski, Appl. Phys. Lett. **94**, 202505 (2009).
[20] L.-P. Carignan, T. Kodera, A. Yelon, D. Ménard, and C. Caloz, *Proceedings of the 39th European Microwave Conference, Rome* (IEEE Press, Piscataway, NJ, 2009), pp. 743–746.
[21] J.-R. Liu, M. Itoh, M. Terada, T. Horikawa, and K.-I. Machida, Appl. Phys. Lett. **91**, 093101 (2007).
[22] L. Qiao, X. Han, B. Gao, J. Wang, F. Wen, and F. Li, J. Appl. Phys. **105**, 053911 (2009).
[23] S. Melle, J. L. Menéndez, G. Armelles, D. Navas, M. Vázquez, K. Nielsch, R. B. Wehrspohn, and U. Gösele, Appl. Phys. Lett.

83, 4547 (2003).
[24] J. González-Díaz, A. García-Martín, G. Armelles, D. Navas, M. Vázquez, K. Nielsch, R. Wehrspohn, and U. Gösele, Adv. Mater. **19**, 2643 (2007).
[25] N. García and E. V. Ponizovskaia, Phys. Rev. E **71**, 046611 (2005).
[26] Y.-S. Zhou, B.-Y. Gu, and F.-H. Whang, Europhys. Lett. **75**, 737 (2006).
[27] J. Chen, D. Tang, B. Zhang, Y. Yang, M. Lu, H. Lu, F. Lu, and W. Xu, J. Appl. Phys. **102**, 023106 (2007).
[28] E. Demirel, A. C. Basaran, and B. Aktas, Eur. Phys. J. B **69**, 173 (2009).
[29] H. García-Miquel, J. Carbonell, V. E. Boria, and J. Sánchez-Dehesa, Appl. Phys. Lett. **94**, 054103 (2009).
[30] J. Carbonell, H. García-Miquel, and J. Sánchez-Dehesa, Phys. Rev. B **81**, 024401 (2010).
[31] A. Encinas-Oropesa, M. Demand, L. Piraux, I. Huynen, and U. Ebels, Phys. Rev. B **63**, 104415 (2001).
[32] M. Demand, A. Encinas-Oropesa, S. Kenane, U. Ebels, I. Huynen, and L. Piraux, J. Magn. Magn. Mater. **249**, 228 (2002).
[33] C. A. Ramos, E. Vassallo Brigneti, and M. Vázquez, Physica B **354**, 195 (2004).
[34] I. Dumitru, F. Li, J. B. Wiley, D. Cimpoesu, A. Stancu, and L. Spinu, IEEE Trans. Magn. **41**, 3361 (2005).
[35] L.-P. Carignan, C. Lacroix, A. Ouimet, M. Ciureanu, A. Yelon, and D. Ménard, J. Appl. Phys. **102**, 023905 (2007).
[36] R. Arias and D. L. Mills, Phys. Rev. B **63**, 134439 (2001).
[37] Z. K. Wang, M. H. Kuok, S. C. Ng, D. J. Lockwood, M. G. Cottam, K. Nielsch, R. B. Wehrspohn, and U. Gösele, Phys. Rev. Lett. **89**, 027201 (2002).
[38] R. Arias and D. L. Mills, Phys. Rev. B **67**, 094423 (2003).
[39] A. A. Stashkevich *et al.*, Phys. Rev. B **80**, 144406 (2009).
[40] A. G. Gurevich and G. A. Melkov, *Magnetization Oscillations and Waves* (CRC Press, Boca Raton, 1996).
[41] L. D. Landau and E. M. Lifshitz, *Electrodynamics of Continuous Media*, 1st ed. (Pergamon, Oxford, 1960).
[42] M. Maryško, Phys. Status Solidi A **47**, 277 (1978).
[43] L. Kraus, Czech. J. Phys., Sect. B **32**, 1264 (1982).
[44] A. Sihvola, *Electromagnetic Mixing Formulas and Applications* (Institution of Electrical Engineers, London, 1999).
[45] V. B. Bregar and M. Pavlin, J. Appl. Phys. **95**, 6289 (2004).
[46] V. B. Bregar, Phys. Rev. B **71**, 174418 (2005).
[47] J. Ramprecht and D. Sjöberg, J. Phys. D **41**, 135005 (2008).
[48] L. Lewin, Proc. Inst. Electr. Eng. **94**, 65 (1947).
[49] N. A. Khizhnyak, Sov. Phys. Tech. Phys. **27**, 2006 (1957).
[50] N. A. Khizhnyak, Sov. Phys. Tech. Phys. **29**, 604 (1959).
[51] C. A. Grimes and D. M. Grimes, Phys. Rev. B **43**, 10780 (1991).
[52] D. Rousselle, A. Berthault, O. Acher, J. P. Bouchaud, and P. G. Zérah, J. Appl. Phys. **74**, 475 (1993).
[53] L. Olmedo, G. Chateau, C. Deleuze, and J. L. Forveille, J. Appl. Phys. **73**, 6992 (1993).
[54] R. G. Geyer, J. Mantese, and J. Baker-Jarvis, NIST Tech. Note **1371** (1994).
[55] E. Matagne, IEEE Trans. Magn. **31**, 1464 (1995).
[56] A. K. Sarychev, R. C. McPhedran, and V. M. Shalaev, Phys. Rev. B **62**, 8531 (2000).
[57] R. Ramprasad, P. Zurcher, M. Petras, M. Miller, and P. Renaud, J. Appl. Phys. **96**, 519 (2004).
[58] L. Z. Wu, J. Ding, H. B. Jiang, C. P. Neo, L. F. Chen, and C. K. Ong, J. Appl. Phys. **99**, 083905 (2006).
[59] O. Acher and S. Dubourg, Phys. Rev. B **77**, 104440 (2008).
[60] A. N. Lagarkov and K. N. Rozanov, J. Magn. Magn. Mater. **321**, 2082 (2009).
[61] O. Klein, S. Donovan, M. Dressel, and G. Grüner, Int. J. Infrared Millim. Waves **14**, 2423 (1993).
[62] R. C. Jones, Phys. Rev. **68**, 93 (1945).
[63] A. D. Berk and B. A. Lengyel, Proc. IRE **43**, 1587 (1955).
[64] C. Kittel, Phys. Rev. **73**, 155 (1948).
[65] M. E. Brodwin and M. K. Parsons, J. Appl. Phys. **36**, 494 (1965).
[66] D. Ménard, M. Britel, P. Ciureanu, and A. Yelon, J. Appl. Phys. **84**, 2805 (1998).
[67] M. S. Wheeler, J. S. Aitchison, and M. Mojahedi, Phys. Rev. B **72**, 193103 (2005).
[68] R. A. Waldron, Br. J. Appl. Phys. **14**, 700 (1963).
[69] N. Bloembergen, J. Appl. Phys. **23**, 1383 (1952).
[70] J. A. Osborn, Phys. Rev. **67**, 351 (1945).
[71] D. Ménard and A. Yelon, J. Appl. Phys. **88**, 379 (2000).
[72] Y. Wu, J. Li, Z.-Q. Zhang, and C. T. Chan, Phys. Rev. B **74**, 085111 (2006).
[73] X. Hu, C. T. Chan, J. Zi, M. Li, and K.-M. Ho, Phys. Rev. Lett. **96**, 223901 (2006).
[74] P. Sheng, *Introduction to Wave Scattering, Localization, and Mesoscopic Phenomena* (Academic, San Diego, 1995).
[75] L.-P. Carignan, V. Boucher, T. Kodera, C. Caloz, A. Yelon, and D. Ménard, Appl. Phys. Lett. **95**, 062504 (2009).
[76] V. Boucher, L.-P. Carignan, T. Kodera, C. Caloz, A. Yelon, and D. Ménard, Phys. Rev. B **80**, 224402 (2009).
[77] A. K. Sarychev and V. M. Shalaev, Phys. Rep. **335**, 275 (2000).
[78] R.-L. Chern and Y.-T. Chen, Phys. Rev. B **80**, 075118 (2009).
[79] A. J. Newell, W. Williams, and D. J. Dunlop, J. Geophys. Res. **98**, 9551 (1993).
[80] J. R. Eshbach, J. Appl. Phys. **34**, 1298 (1963).
[81] U. Netzelmann, J. Appl. Phys. **68**, 1800 (1990).
[82] J. Dubowik, Phys. Rev. B **54**, 1088 (1996).
[83] G. N. Kakazei, A. F. Kravets, N. A. Lesnik, M. M. Pereira de Azevedo, Y. G. Pogorelov, and J. B. Sousa, J. Appl. Phys. **85**, 5654 (1999).
[84] I. Dumitru, D. D. Sandu, and C. G. Verdes, Phys. Rev. B **66**, 104432 (2002).
[85] D. S. Schmool, R. Rocha, J. B. Sousa, J. A. M. Santos, G. N. Kakazei, J. S. Garitaonandia, and L. Lezama, J. Appl. Phys. **101**, 103907 (2007).
[86] R. Skomski, G. C. Hadjipanayis, and D. J. Sellmyer, IEEE Trans. Magn. **43**, 2956 (2007).
[87] S. E. Lofland, H. García-Miquel, M. Vázquez, and S. M. Bhagat, J. Appl. Phys. **92**, 2058 (2002).
[88] J. Lam, J. Appl. Phys. **60**, 4230 (1986).
[89] C. L. Holloway, E. F. Kuester, J. Baker-Jarvis, and P. Kabos, IEEE Trans. Antennas Propag. **51**, 2596 (2003).
[90] L. Jylhä, I. Kolmakov, S. Maslovski, and S. Tretyakov, J. Appl. Phys. **99**, 043102 (2006).
[91] J. A. Schuller, R. Zia, T. Taubner, and M. L. Brongersma, Phys. Rev. Lett. **99**, 107401 (2007).
[92] L. Peng, L. Ran, H. Chen, H. Zhang, J. A. Kong, and T. M. Grzegorczyk, Phys. Rev. Lett. **98**, 157403 (2007).
[93] Q. Zhao, L. Kang, B. Du, H. Zhao, Q. Xie, X. Huang, B. Li, J. Zhou, and L. Li, Phys. Rev. Lett. **101**, 027402 (2008).
[94] F. Zhang, Q. Zhao, L. Kang, J. Zhou, and D. Lippens, Phys. Rev.

B **80**, 195119 (2009).
[95] E. Schloemann, J. Magn. Magn. Mater. **209**, 15 (2000).
[96] W. S. Ament and G. T. Rado, Phys. Rev. **97**, 1558 (1955).
[97] L. Kraus, J. Magn. Magn. Mater. **195**, 764 (1999).
[98] R. I. Joseph and E. Schlömann, J. Appl. Phys. **32**, 1001 (1961).
[99] S. Rajagopalan and J. K. Furdyna, Phys. Rev. B **39**, 2532 (1989).
[100] C. D. Cantrell, *Modern Mathematical Methods for Physicists and Engineers* (Cambridge University Press, Cambridge, 2000).
[101] H. C. van de Hulst, *Light Scattering by Small Particles* (Wiley, New York, 1957).